

UNIVERSIDAD DE CONCEPCIÓN



CENTRO DE INVESTIGACIÓN EN
INGENIERÍA MATEMÁTICA (CI²MA)



On the discontinuous Galerkin method for solving boundary
problems for the Helmholtz equation: A priori and a posteriori
error analyses

TOMÁS BARRIOS, ROMMEL BUSTINZA,
VÍCTOR DOMÍNGUEZ

PREPRINT 2013-23

SERIE DE PRE-PUBLICACIONES

On the discontinuous Galerkin method for solving boundary problems for the Helmholtz equation: A priori and a posteriori error analyses*

TOMÁS P. BARRIOS[†] ROMMEL BUSTINZA[‡] and VÍCTOR DOMÍNGUEZ[§]

Abstract

We apply the local discontinuous Galerkin (LDG for short) method to solve a mixed boundary value problems for the Helmholtz equation in bounded polygonal domain in 2D. Under some assumptions on regularity of the solution of an adjoint problem, we prove that: (a) the corresponding indefinite discrete scheme is well posed; (b) there is convergence with the expected convergence rates as long as the meshsize h is small enough. We give precise information on how small h has to be in terms of the size of the wavenumber and its distance to the set of eigenvalues for the same boundary value problem for the Laplacian. We also present an a posteriori error estimator showing both the reliability and efficiency of the estimator complemented with detailed information on the dependence of the constants on the wavenumber. We finish presenting extensive numerical experiments which illustrate the theoretical results proven in this paper and suggest that stability and convergence may occur under less restrictive assumptions than those taken in the present work.

Key words: LDG, Helmholtz problem, indefinite bilinear forms.

Mathematics subject classifications (1991): 65N30; 65N12; 65N15

1 Introduction

In this paper we are interested in the numerical analysis of discontinuous Galerkin (dG) schemes for the following model boundary value problem for the Helmholtz equation:

$$-\Delta u - \omega^2 u = f \quad \text{in } \Omega, \quad u = g_D \quad \text{on } \Gamma_D, \quad \text{and} \quad \partial_{\nu} u = g_N \quad \text{on } \Gamma_N. \quad (1)$$

Here, Ω is a bounded polygonal Lipschitz domain in \mathbb{R}^2 , whose boundary $\Gamma := \partial\Omega$ is decomposed into two disjoint sets Γ_D and Γ_N (that is $\Gamma = \bar{\Gamma}_D \cup \bar{\Gamma}_N$), with $|\Gamma_D| > 0$, and $\omega > 0$ denotes a fixed wave number (of corresponding wave length $\lambda = 2\pi/\omega$). The right hand side f is a source term in $L^2(\Omega)$, while the boundary data $g_D \in H^{1/2}(\Gamma_D)$ and $g_N \in L^2(\Gamma_N)$, and ν represents the outward normal unit vector to Γ .

Now, introducing the auxiliary unknown $\sigma := \nabla u$, problem (1) is rewritten as: *Find (σ, u) in appropriate spaces, such that*

$$\begin{aligned} \sigma &= \nabla u \quad \text{in } \Omega, \quad -\operatorname{div} \sigma - \omega^2 u = f \quad \text{in } \Omega, \\ u &= g_D \quad \text{on } \Gamma_D, \quad \text{and} \quad \sigma \cdot \nu = g_N \quad \text{on } \Gamma_N. \end{aligned} \quad (2)$$

*This research was partially supported by Spanish Project MTM2010-21037, the Dirección de Investigación of the Universidad Católica de la Santísima Concepción, FONDECYT project No. 1130158, BASAL project CMM, Universidad de Chile; Centro de Investigación en Ingeniería Matemática (CI²MA), Universidad de Concepción; and CONICYT through project Anillo ACT1118 (ANANUM).

[†]Departamento de Matemática y Física Aplicadas, Universidad Católica de la Santísima Concepción, Casilla 297, Concepción, Chile, e-mail: tomas@ucsc.cl

[‡]CI²MA and Departamento de Ingeniería Matemática, Universidad de Concepción, Casilla 160-C, Concepción, Chile, e-mail: rbustinz@ing-mat.udec.cl

[§]Departamento de Ingeniería Matemática e Informática, Universidad Pública de Navarra, Campus de Tudela, 31500 - Tudela, Spain, e-mail: victor.dominguez@unavarra.es

The use of classical continuous Galerkin finite element method provides good phase and amplitude accuracy as long as the mesh is fine enough with respect to the wave number in the propagation region. This condition could be too expensive even for moderate wave numbers. Thus, one of the main concerns in acoustic finite element analysis is the adequacy of the finite element mesh. Acousticians often use the so-called *rule of the thumb* (see [31]) which prescribes a relation between the minimal number of elements and the wave number. Indeed, using linear finite elements, an estimate of the relative error is derived, which is of the form: $e_h \leq C_1\omega h + C_2\omega^3 h^2$, $\omega h < 1$, and where the constants $C_1, C_2 > 0$ are independent of the wave number ω and the mesh size h . The first term on the right hand side of the previous estimate denotes the interpolation error while the second one represents the *pollution effect*. It is clear that the interpolation error would be constant if ωh remains constant. However, this choice does not guarantee the control of the pollution effect, that increases with ω . This behavior has become a real challenge for numerical analysts and therefore several different approaches to deal with the pollution effect have been developed (see for e.g. [16, 17, 31] and the references therein). In [24, 12, 35], the authors introduce discontinuous methods for the acoustic problem considering non polygonal basis functions. They use wave like functions in order to better capture the unique features corresponding to medium and high frequency regime.

In the context of discontinuous Galerkin methods (see [1] for an overview) there have been several approaches to deal with this problem, too. In [23, 26] the authors develop a discontinuous Galerkin method for Helmholtz equation in two dimensions, using local plane waves as trial and test functions. Our aim here is similar to them, but using piecewise polynomial finite element basis as starting point to keep the simplicity of coding. There are previous works in this direction, such as [7, 34], where the authors propose two very similar DG schemes for solving (1), and include several numerical examples, showing a good behavior of the discrete solution for different values of the wave number ω , by choosing appropriately the parameters that define the method as well as taking into account the *rule of the thumb* $\omega h < 1$. However, up to the authors' knowledge, they do not establish (from a theoretical point of view) neither the well-posedness of the scheme nor its corresponding a priori error estimate. On the other hand, in [18] the authors applied a stabilized Interior Penalty Discontinuous Galerkin (IPDG) method to the Helmholtz equation with the first order absorbing boundary conditions (cf. [15]) instead of the mixed boundary conditions considered here. Later, in [19], they extend their analysis to the corresponding *hp*- version, proving optimal convergence with respect to h in the high frequency regime, when a mesh condition is satisfied.

Therefore, we are interested in deriving the LDG formulation of (2) and establish that it has a unique solution as well as the optimal rates of convergence (under suitable additional regularity on the exact solution), for moderated values of wave number. This is done following the ideas given in [28], for solving an indefinite time-harmonic Maxwell problem, and are based on an earlier work of Schatz ([38]). Then, we develop (in essence) the a priori error analysis applying duality arguments, so the existence and uniqueness of the solution of the discrete scheme is proven for h *small enough*. The minimum size of h to enter in the convergence region is shown to depend on the size of ω , the distance to the closest eigenvalue for the Laplacian and on the regularity of the adjoint problem (see Hypothesis 1.1 below).

Another important aspect to take into account is the development of a technique that improves the quality of numerical approximation, without performing uniform refinement. One tool is the so called a posteriori error analysis, which gives us a full computable indicator that behaves as the exact error and thus is used in the subsequent adaptive algorithm. For this reason, this indicator is known as a posteriori error estimator. In the context of DG methods, we can refer to [2, 6, 10, 29, 32, 37], where several a posteriori error analyses are developed for standard second order elliptic boundary value problems. Up to the authors' knowledge, there are few work on a posteriori error estimation using DG methods for Helmholtz problem. We can mention [27], which includes an a posteriori error estimation and a convergence analysis of the adaptive mechanism when applying an IPDG approach to deal with Helmholtz boundary value problems with the first order absorbing boundary conditions. Then, as complementary part of the current analysis, we derive a reliable and quasi-efficient a posteriori error estimate, in order to improve the quality of the numerical approximation, showing the dependence of the constants on the frequency ω .

The outline of the paper is as follows: in Section 2 we introduce the main elements that let us to derive the LDG formulation associated to (2), reviewing some basic properties of the discrete scheme.

The well-posedness of the scheme as well as the corresponding a priori error bounds are stated at the end of this section; the proofs of these results are carried out in Section 3. Next, in Section 4 we derive a residual a posteriori error estimate, which results to be reliable and locally efficient, up to high order terms. Finally, we show several numerical examples in Section 5, validating our theoretical results, and summarize the work presented in this paper, drawing some conclusions.

Hypothesis 1.1 *Given $z \in L^2(\Omega)$ we will assume that the problem*

$$-\Delta\varphi - \omega^2\varphi = z, \quad \text{on } \Omega \quad \varphi|_{\Gamma_D} = 0, \quad \partial_\nu\varphi|_{\Gamma_N} = 0. \quad (3)$$

admits a unique solution, i.e., $-\omega^2$ is not an eigenvalue for the Laplacian.

We demand also an extra smoothness properties for \mathcal{L}_ω : There exists $\varepsilon \in (1/2, 1]$ such that the mapping

$$\begin{aligned} \mathcal{L}_\omega : L^2(\Omega) &\longrightarrow H^{1+\varepsilon}(\Omega) \\ z &\longmapsto \varphi \end{aligned} \quad (4)$$

is continuous ($H^t(\Omega)$ denotes the classical Sobolev space of order t).

We point out that this hypothesis implies in particular that problem (1) is well posed. Regarding (4), it is well known that such result holds for the pure Dirichlet and Neumann problem. With mixed boundary conditions this hypothesis is satisfied if one assumes some geometric restrictions on the angles between the sides of Γ_D and Γ_N . We refer to [25, Chapter 4] or [14] for more references on this topic.

Remark 1.2 Although the boundary problem (1) admits complex-valued data functions f , g_D and g_N , actually this is what one can expect in many practical applications, we assume for lighten the analysis that all these functions, and so the solution, are real valued. The results can be straightforwardly adapted to the complex case.

For similar reasons, we will assume that $\Gamma_D \neq \emptyset$. The pure Neumann problem can be studied with a slight modification of the arguments developed here (see Remark 3.6 for more information on this topic). \square

2 The LDG formulation

In this section, we partially follow [30] (see also [3] and [4]) to derive a discrete formulation for the linear model (2), applying a consistent and conservative discontinuous Galerkin method in gradient form.

2.1 Meshes, averages, and jumps

We let $\{\mathcal{T}_h\}_{h>0}$ be a family of shape-regular triangulations of $\bar{\Omega}$ (with possible hanging nodes) made up of straight-side triangles T with diameter h_T and unit outward normal vector to ∂T given by ν_T . As usual, the index h also denotes

$$h := \max_{T \in \mathcal{T}_h} h_T,$$

which without loss of generality we can assume to be less than 1.

Given \mathcal{T}_h , its edges are defined as follows. An *interior edge* of \mathcal{T}_h is the (nonempty) interior of $\partial T \cap \partial T'$, where T and T' are two adjacent elements of \mathcal{T}_h , not necessarily matching. Similarly, a *boundary edge* of \mathcal{T}_h is the (nonempty) interior of $\partial T \cap \partial\Omega$, where T is a boundary element of \mathcal{T}_h . We denote by \mathcal{E}_I the list of all interior edges of (counted only once) on Ω , and by \mathcal{E}_D and \mathcal{E}_N the lists of all edges lying on Γ_D and Γ_N . Hence, $\mathcal{E} := \mathcal{E}_I \cup \mathcal{E}_D \cup \mathcal{E}_N$ is the set of all edges, or skeleton, of the triangulation \mathcal{T}_h . Further, for each $e \in \mathcal{E}$, h_e represents its length. Also, in what follows we assume that \mathcal{T}_h is of *bounded variation*, which means that there exists a constant $c > 1$, independent of the meshsize h , such that

$$c^{-1} \leq \frac{h_T}{h_{T'}} \leq c$$

for each pair $T, T' \in \mathcal{T}_h$ sharing an interior edge.

Next, to define average and jump operators, let T and T' be two adjacent elements of \mathcal{T}_h and \mathbf{x} be an arbitrary point on the interior edge $e = \partial T \cap \partial T' \in \mathcal{E}_I$. In addition, let v and $\boldsymbol{\tau}$ be scalar- and vector-valued functions, respectively, that are smooth inside each element $T \in \mathcal{T}_h$. We denote by $(v_{T,e}, \boldsymbol{\tau}_{T,e})$ the restriction of $(v_T, \boldsymbol{\tau}_T)$ to e . Then, we define the averages at $\mathbf{x} \in e$ by:

$$\{v\} := \frac{1}{2}(v_{T,e} + v_{T',e}), \quad \{\boldsymbol{\tau}\} := \frac{1}{2}(\boldsymbol{\tau}_{T,e} + \boldsymbol{\tau}_{T',e}).$$

Similarly, the jumps at $\mathbf{x} \in e$ are given by

$$[[v]] := v_{T,e} \boldsymbol{\nu}_T + v_{T',e} \boldsymbol{\nu}_{T'}, \quad [[\boldsymbol{\tau}]] := \boldsymbol{\tau}_{T,e} \cdot \boldsymbol{\nu}_T + \boldsymbol{\tau}_{T',e} \cdot \boldsymbol{\nu}_{T'}.$$

On boundary edges e , we set $\{v\} := v$, $\{\boldsymbol{\tau}\} := \boldsymbol{\tau}$, as well as $[[v]] := v \boldsymbol{\nu}$, and $[[\boldsymbol{\tau}]] := \boldsymbol{\tau} \cdot \boldsymbol{\nu}$. Hereafter, as usual, ∇_h denotes the piecewise gradient operator.

2.2 LDG method

Our purpose is to approximate the exact solution $(\boldsymbol{\sigma}, u)$ of (2) by discrete functions $(\boldsymbol{\sigma}_h, u_h)$ in appropriate finite element space $\boldsymbol{\Sigma}_h \times V_h$, defined as follows

$$\begin{aligned} V_h &:= \{v_h \in L^2(\Omega) : v|_T \in \mathbb{P}_m(T), \quad \forall T \in \mathcal{T}_h\}, \\ \boldsymbol{\Sigma}_h &:= \{\boldsymbol{\tau}_h \in [L^2(\Omega)]^2 : \boldsymbol{\tau}_h|_T \in [\mathbb{P}_{m'}(T)]^2, \quad \forall T \in \mathcal{T}_h\}. \end{aligned}$$

In the expression above $\mathbb{P}_m(T)$ denotes the space of polynomials on T of degree m . We restrict ourselves to consider $m \leq m' + 1$ so that $\nabla_h V_h \subset \boldsymbol{\Sigma}_h$, which is required for guaranteeing the solvability of the discrete variational formulation. The usual choices in practical situations is letting $m' = m$ or $m' = m - 1$.

We are ready to introduce the DG method: find $(\boldsymbol{\sigma}_h, u_h) \in \boldsymbol{\Sigma}_h \times V_h$ so that for all $T \in \mathcal{T}_h$ it satisfies

$$\begin{aligned} \int_T \boldsymbol{\sigma}_h \cdot \boldsymbol{\tau} + \int_T u_h \operatorname{div} \boldsymbol{\tau} - \int_{\partial T} \hat{u} \boldsymbol{\tau} \cdot \boldsymbol{\nu}_T &= 0 \quad \forall \boldsymbol{\tau} \in \boldsymbol{\Sigma}_h, \\ \int_T \boldsymbol{\sigma}_h \cdot \nabla v - \int_{\partial T} v \hat{\boldsymbol{\sigma}} \cdot \boldsymbol{\nu}_T - \omega^2 \int_T u_h v &= \int_T f v \quad \forall v \in V_h. \end{aligned} \tag{5}$$

The functions \hat{u} and $\hat{\boldsymbol{\sigma}}$ are the so called *numerical fluxes* and depend on $u_h, \boldsymbol{\sigma}_h$, the boundary data, and are set so that some compatibility conditions are satisfied (see [1]).

Indeed, taking into account the approach from [36] and [11], the LDG is defined by taking $\hat{u} := \hat{u}(u_h, g_D)$ and $\hat{\boldsymbol{\sigma}} := \hat{\boldsymbol{\sigma}}(\boldsymbol{\sigma}_h, u_h, g_D, g_N)$ for each $T \in \mathcal{T}_h$ as follows:

$$\hat{u}_{T,e} := \begin{cases} \{u_h\} + [[u_h]] \cdot \boldsymbol{\beta} & \text{if } e \in \mathcal{E}_I, \\ g_D & \text{if } e \in \mathcal{E}_D, \\ u_h & \text{if } e \in \mathcal{E}_N, \end{cases} \tag{6}$$

and

$$\hat{\boldsymbol{\sigma}}_{T,e} := \begin{cases} \{\boldsymbol{\sigma}_h\} - [[\boldsymbol{\sigma}_h]] \boldsymbol{\beta} - \alpha [[u_h]] & \text{if } e \in \mathcal{E}_I, \\ \boldsymbol{\sigma}_h - \alpha (u_h - g_D) \boldsymbol{\nu} & \text{if } e \in \mathcal{E}_D, \\ g_N \boldsymbol{\nu} & \text{if } e \in \mathcal{E}_N, \end{cases} \tag{7}$$

where the auxiliary functions α (scalar) and $\boldsymbol{\beta}$ (vector), to be chosen appropriately, are single valued on each edge $e \in \mathcal{E}$ and such that they allow us to prove the optimal rates of convergence of our approximation. To this aim, we set $\alpha := \frac{\hat{\alpha}}{\mathbf{h}}$, and $\boldsymbol{\beta}$ as an arbitrary vector in \mathbb{R}^2 . Hereafter, $\hat{\alpha} > 0$ is fixed, while \mathbf{h} is defined on the skeleton of \mathcal{T}_h by

$$\mathbf{h}_e := \begin{cases} \max\{h_T, h_{T'}\} & \text{if } e \in \mathcal{E}_I, \\ h_T & \text{if } e \in \mathcal{E}_\Gamma. \end{cases}$$

Then, integrating by parts in the first equation in (5) and summing up over all $T \in \mathcal{T}_h$, we arrive to the problem: Find $(\boldsymbol{\sigma}_h, u_h) \in \boldsymbol{\Sigma}_h \times V_h$ such that:

$$\int_{\Omega} \boldsymbol{\sigma}_h \cdot \boldsymbol{\tau} - \int_{\Omega} \nabla_h u_h \cdot \boldsymbol{\tau} + S_h(u_h, \boldsymbol{\tau}) = \int_{\Gamma_D} g_D \boldsymbol{\tau} \cdot \boldsymbol{\nu}, \quad (8)$$

$$\int_{\Omega} \nabla_h v \cdot \boldsymbol{\sigma}_h - S_h(v, \boldsymbol{\sigma}_h) + \boldsymbol{\alpha}(u_h, v) - \omega^2 \int_{\Omega} u_h v = \int_{\Omega} f v + \int_{\Gamma_D} \alpha g_D v + \int_{\Gamma_N} g_N v,$$

for all $(\boldsymbol{\tau}, v) \in \boldsymbol{\Sigma}_h \times V_h$, where the bilinear forms appearing above are given by

$$S_h(v, \boldsymbol{\tau}) := \int_{\mathcal{E}_I} (\{\boldsymbol{\tau}\} - \llbracket \boldsymbol{\tau} \rrbracket \boldsymbol{\beta}) \cdot \llbracket v \rrbracket + \int_{\mathcal{E}_D} v \boldsymbol{\tau} \cdot \boldsymbol{\nu}, \quad (9)$$

$$\boldsymbol{\alpha}(v, w) := \int_{\mathcal{E}_I} \alpha \llbracket v \rrbracket \cdot \llbracket w \rrbracket + \int_{\mathcal{E}_D} \alpha v w. \quad (10)$$

2.3 Sobolev and discrete norms

We denote by $\|\cdot\|_{0,\Omega}$ the standard $L^2(\Omega)$ norm. Sobolev spaces $H^r(\Omega)$ will appear in what follows, equipped with the norm

$$\|v\|_{r,\Omega}^2 := \|v\|_{0,\Omega}^2 + \sum_{|\boldsymbol{\beta}|=r} \|\partial^{\boldsymbol{\beta}} v\|_{0,\Omega}^2,$$

for positive integer r (we follow the usual multi-index notation). For fractional values of $r = n + \gamma$, with $n \in \mathbb{N} \cup \{0\}$ and $\gamma \in (0, 1)$, we have instead the norm

$$\|v\|_{r,\Omega}^2 := \|v\|_{0,\Omega}^2 + \sum_{|\boldsymbol{\beta}|=n} |\partial^{\boldsymbol{\beta}} v|_{\gamma,\Omega}^2,$$

where

$$|f|_{\gamma,\Omega}^2 := \int_{\Omega} \int_{\Omega} \frac{|f(\mathbf{x}) - f(\mathbf{y})|^2}{|\mathbf{x} - \mathbf{y}|^{2+2\gamma}} d\mathbf{x} d\mathbf{y}$$

is the Slobodecki seminorm. Finally, the tensor Sobolev spaces $H^r(\Omega) \times H^r(\Omega)$ will be equipped with the usual norm and denoted with the same symbol $\|\cdot\|_{r,\Omega}$, to avoid any confusion in the context.

The space $L^2(e)$, with e being a edge or a finite union of edges, is defined accordingly and we will use the same notation for the norm, namely, $\|\cdot\|_{0,e}$.

Finally, $H^1(\mathcal{T}_h)$ denotes the space whose the elements $v|_T \in H^1(T)$, for all $T \in \mathcal{T}_h$. We endow this space with the discrete seminorm and norm (see [8])

$$|v|_h := \left(\|\alpha^{1/2} \llbracket v \rrbracket\|_{0,\mathcal{E}_I}^2 + \|\alpha^{1/2} v\|_{0,\mathcal{E}_D}^2 \right)^{1/2} \quad \forall v \in H^1(\mathcal{T}_h), \quad (11)$$

and

$$\|v\|_h^2 := \|\nabla_h v\|_{0,\Omega}^2 + |v|_h^2 \quad \forall v \in H^1(\mathcal{T}_h). \quad (12)$$

We point out that a Poincaré type inequality (see [9] for a proof) holds: there exists $C_P > 0$, independent of \mathcal{T}_h , such that

$$\|v\|_{0,\Omega} \leq C_P \|v\|_h \quad \forall v \in H^1(\mathcal{T}_h). \quad (13)$$

3 Convergence and stability of LDG method

This section is devoted to proving the a priori error estimate for the method.

Theorem 3.1 *There exists $h_0 = h_0(\varepsilon, \omega) > 0$ such that for all $h < h_0$ the numerical method (20) admits a unique solution $u_h \in V_h$. Moreover if $u \in H^{l+1}(\Omega)$ with $1/2 < l \leq m$, there holds*

$$\|u_h - u\|_h + \|\boldsymbol{\sigma}_h - \nabla u\|_{0,\Omega} \leq C(\varepsilon, \omega) \left[\sum_{T \in \mathcal{T}_h} h_T^{2l} \|u\|_{l+1,T}^2 \right]^{1/2},$$

with $C(\varepsilon, \omega) > 0$ independent of h and u .

The proof is presented in the next subsections. We stress that $C(\varepsilon, \omega)$ and $h_0(\varepsilon, \omega)$ is shown to be dependent (see (28)-(29)) on ω , via how large and how close it is from the closest eigenvalue for the Laplacian, and the regularity of the adjoint problem (3), represented by the parameter ε .

Hence, we start recalling some well-known results which we present for the sake of completeness and give, in the last part, the proof itself.

3.1 Approximation properties of the discrete spaces

We start recalling the local approximation properties of piecewise polynomials. Denote by $\Pi_T^m : L^2(T) \rightarrow \mathbb{P}_m$ the L^2 -orthogonal projection. Then there exists $C > 0$, independent of the meshsize, such that for each s, t satisfying $0 \leq s \leq m+1$ and $0 \leq s < t$, there holds (cf. [13] and [21])

$$|w - \Pi_T^m w|_{s,T} \leq C h_T^{\min\{t, m+1\} - s} \|w\|_{t,T} \quad \forall w \in H^t(T), \quad (14)$$

and

$$|w - \Pi_T^m w|_{0,\partial T} \leq C h_T^{\min\{t, m+1\} - 1/2} \|w\|_{t,T} \quad \forall w \in H^t(T). \quad (15)$$

Therefore, if

$$\Pi_{V_h} : L^2(\Omega) \rightarrow V_h, \quad \Pi_{\Sigma_h} : [L^2(\Omega)]^2 \rightarrow \Sigma_h,$$

are the L^2 -orthogonal projections on the discrete spaces V_h and Σ_h , respectively, we have, from (14)-(15):

$$\|v - \Pi_{V_h} v\|_{0,\Omega} \leq C_l \left[\sum_{T \in \mathcal{T}_h} h_T^{2l} \|v\|_{l,T}^2 \right]^{1/2}, \quad \text{and} \quad \|v - \Pi_{V_h} v\|_h \leq C_l \left[\sum_{T \in \mathcal{T}_h} h_T^{2l-2} \|v\|_{l,T}^2 \right]^{1/2}, \quad (16)$$

for $v \in H^l(\mathcal{T}_h)$, $1 \leq l \leq m+1$, with $C_l > 0$ independent of v , σ and \mathcal{T}_h . Similarly, we obtain

$$\|\Pi_{\Sigma_h} \sigma - \sigma\|_{0,\Omega} \leq C_l \left[\sum_{T \in \mathcal{T}_h} h_T^{2l} \|\sigma\|_{l,T}^2 \right]^{1/2},$$

for $\sigma \in [H^l(\mathcal{T}_h)]^2$, with $1 \leq l \leq m'+1$.

3.2 The primal formulation of the LDG method

Associated to S_h (cf. (9)), we introduce the discrete lifting operators $\mathbf{S}_h : H^1(\mathcal{T}_h) \rightarrow \Sigma_h$ and $\mathbf{G}_h : L^2(\Gamma_D) \rightarrow \Sigma_h$ defined, respectively, as the solutions of the problems

$$\int_{\Omega} \mathbf{S}_h(v) \cdot \tau = S_h(v, \tau) \quad \forall \tau \in \Sigma_h, \quad (17)$$

$$\int_{\Omega} \mathbf{G}_h(g_D) \cdot \tau = \int_{\Gamma_D} g_D \tau \cdot \nu \quad \forall \tau \in \Sigma_h, \quad (18)$$

whose existence and uniqueness are guaranteed by Riesz representation theorem. We notice in passing that if $v \in H^1(\Omega)$ with $v|_{\Gamma_D} = g_D$, then $\mathbf{G}_h(g_D) = \mathbf{S}_h(v)$.

Thus, the first equation of (8) can be read as

$$\int_{\Omega} \sigma_h \cdot \tau = \int_{\Omega} (\nabla_h u_h - \mathbf{S}_h(u_h) + \mathbf{G}_h(g_D)) \cdot \tau \quad \forall \tau \in \Sigma_h.$$

Since $\nabla_h V_h \subset \Sigma_h$, we conclude

$$\sigma_h = \nabla_h u_h - \mathbf{S}_h(u_h) + \mathbf{G}_h(g_D). \quad (19)$$

In other words, we have expressed σ_h in terms of u_h and the Dirichlet data. Besides, from the second equation of (8), taking into account again \mathbf{S}_h , we obtain

$$\int_{\Omega} \sigma_h \cdot \nabla_h v + \alpha(u_h, v) - \int_{\Omega} \mathbf{S}_h(v) \cdot \sigma_h - \omega^2 \int_{\Omega} u_h v = \int_{\Omega} f v + \int_{\Gamma_N} g_N v + \int_{\Gamma_D} \alpha g_D v.$$

Using (19) to substitute σ_h we arrive to the reduced (an equivalent) primal form: Find $u_h \in V_h$ such that

$$a_h(u_h, v) - \omega^2 \int_{\Omega} u_h v = \mathcal{F}_h(v) \quad \forall v \in V_h, \quad (20)$$

where

$$a_h(t, v) := \int_{\Omega} (\nabla_h t - \mathbf{S}_h(t)) \cdot (\nabla_h v - \mathbf{S}_h(v)) + \alpha(t, v), \quad (21)$$

$$\mathcal{F}_h(v) := \int_{\Omega} f v + \int_{\Gamma_N} g_N v + \int_D \alpha g_D v - \int_{\Omega} (\nabla_h v - \mathbf{S}_h(v)) \cdot \mathbf{G}_h(g_D). \quad (22)$$

This way we have established the next result.

Theorem 3.2 *If $(\sigma_h, u_h) \in \Sigma_h \times V_h$ is a solution of (8), then $u_h \in V_h$ is a solution of (20). Reciprocally, if $u_h \in V_h$ is a solution of (20) then $(\sigma_h, u_h) \in \Sigma_h \times V_h$, with $\sigma_h := \nabla_h u_h - \mathbf{S}_h(u_h) + \mathbf{G}_h(g_D)$, is a solution of (8).*

The boundedness and ellipticity of bilinear form a_h is established next.

Theorem 3.3 *There exist $C_{\text{cont}}, c_{\text{coer}} > 0$ such that for all $t, v \in H^1(\mathcal{T}_h)$ there hold*

$$|a_h(t, v)| \leq C_{\text{cont}} \|t\|_h \|v\|_h, \quad \text{and} \quad a_h(v, v) \geq c_{\text{coer}} \|v\|_h^2.$$

Proof. We refer to [36, 9] for a proof of this result. We note that $C_{\text{cont}} := \max\{2, 2\|\mathbf{S}_h\|, \|\mathbf{S}_h\|^2\}$. \square

We point out that this theorem is the key result for proving stability and convergence of the method for the Laplace equation. However, the L^2 -term spoils the coercivity of the bilinear form and forces us to consider a different approach for proving the convergence of the method. This is what we will describe in next subsection.

3.3 Proof of Theorem 3.1

We start assuming that the exact solution $u \in H^{l+1}(\Omega)$ with $l > 1/2$ and that there exists a numerical solution u_h for the reduced primal scheme (20).

Take an arbitrary element $v \in V_h$. Now, thanks to the coercivity of a_h (cf. Theorem 3.3), there holds

$$\begin{aligned} c_{\text{coer}} \|u_h - v\|_h^2 &\leq a_h(u_h - v, u_h - v) = a_h(u_h, u_h - v) - a_h(u, u_h - v) + a_h(u - v, u_h - v) \\ &= R_h(u, u_h - v) + \omega^2 \int_{\Omega} (u_h - u)(u_h - v) + a_h(u - v, u_h - v), \end{aligned} \quad (23)$$

where

$$R_h(u, q) := \mathcal{F}_h(q) - a_h(u, q) + \omega^2 \int_{\Omega} u q \quad \forall q \in V_h,$$

is the so-called *consistency term*. We point out in pass that, unlike the original formulation of the method (5), the consistency term does not vanish for the exact solution u , i.e. the primal formulation is not consistent.

By using the continuity of the bilinear form a_h , we derive from (23) that

$$c_{\text{coer}} \|u_h - v\|_h \leq \sup_{0 \neq z \in V_h} \frac{1}{\|z\|_h} R_h(u, z) + \omega^2 \sup_{0 \neq z \in V_h} \frac{1}{\|z\|_h} \int_{\Omega} (u - u_h) z + C_{\text{cont}} \|u - v\|_h. \quad (24)$$

The first term is bounded straightforwardly by using the following relations [9, 21]

$$R_h(u, z) = S_h(z, \Pi_{\Sigma_h} \nabla u - \nabla u) \leq C_{l,S} \left[\sum_{T \in \mathcal{T}_h} h_T^{2l} |\nabla u|_{l,T}^2 \right]^{1/2} \|z\|_h \quad \forall z \in V_h, \quad (25)$$

which holds for all $1/2 < l \leq m$.

Next we show a simple presentation of the boundedness of second order term in (24). To this aim, we require the following lemma. Recall first the mapping \mathcal{L}_ω introduced in (4).

Lemma 3.4 *Let $z \in L^2(\Omega)$ and u the exact solution of (1). If $u_h \in V_h$ is a solution of (20) then for any $\psi \in V_h$ it holds*

$$\begin{aligned} \int_{\Omega} (u - u_h)z &= a_h(u - u_h, \mathcal{L}_{\omega}z - \psi) + \omega^2 \int_{\Omega} (u - u_h)(\mathcal{L}_{\omega}z - \psi) + S_h(u_h - u, \nabla \mathcal{L}_{\omega}z - \mathbf{\Pi}_{\Sigma_h} \nabla \mathcal{L}_{\omega}z) \\ &\quad + S_h(\psi, \nabla u - \mathbf{\Pi}_{\Sigma_h} \nabla u). \end{aligned}$$

Proof. Fix $z \in L^2(\Omega)$ and set $\varphi := \mathcal{L}_{\omega}z \in H^{1+\varepsilon}(\Omega)$ (recall that $\varepsilon > 1/2$). Take then $v \in H^1(\mathcal{T}_h)$. By integrating by parts on each element of the grid \mathcal{T}_h and using that $[[\nabla\varphi]] = 0$ on any $e \in \mathcal{E}_N \cup \mathcal{E}_I$, we deduce

$$- \int_{\Omega} vz = \int_{\Omega} v(\Delta\varphi + \omega^2\varphi) = - \int_{\Omega} \nabla_h v \cdot \nabla\varphi + \omega^2 \int_{\Omega} v\varphi + \int_{\mathcal{E}_D \cup \mathcal{E}_I} [[v]] \cdot \{\nabla\varphi\}.$$

Besides, since $\varphi|_{\Gamma_D} = 0$, $[[\varphi]] = 0$ for all $e \in \mathcal{E}_D \cup \mathcal{E}_I$,

$$\mathbf{S}_h(\varphi) = \mathbf{0}, \quad \text{and} \quad \boldsymbol{\alpha}(\varphi, v) = 0, \quad \forall v \in H^1(\mathcal{T}_h).$$

Thus

$$\begin{aligned} - \int_{\Omega} vz &= -a_h(v, \varphi) + \omega^2 \int_{\Omega} v\varphi - \int_{\Omega} \mathbf{S}_h(v) \cdot \nabla\varphi + \int_{\mathcal{E}_D \cup \mathcal{E}_I} [[v]] \cdot \{\nabla\varphi\} \\ &= -a_h(v, \varphi) + \omega^2 \int_{\Omega} v\varphi - \int_{\Omega} \mathbf{S}_h(v) \cdot \mathbf{\Pi}_{\Sigma_h} \nabla\varphi + \int_{\mathcal{E}_D \cup \mathcal{E}_I} [[v]] \cdot \{\nabla\varphi\} \\ &= -a_h(v, \varphi) + \omega^2 \int_{\Omega} v\varphi + \int_{\mathcal{E}_D \cup \mathcal{E}_I} [[v]] \cdot \{\nabla\varphi - \mathbf{\Pi}_{\Sigma_h} \nabla\varphi\} + \int_{\mathcal{E}_I} [[\mathbf{\Pi}_{\Sigma_h} \nabla\varphi]] \boldsymbol{\beta} \cdot [[v]] \\ &= -a_h(v, \varphi) + \omega^2 \int_{\Omega} v\varphi + \int_{\mathcal{E}_D \cup \mathcal{E}_I} [[v]] \cdot \{\nabla\varphi - \mathbf{\Pi}_{\Sigma_h} \nabla\varphi\} - \int_{\mathcal{E}_I} [[\nabla\varphi - \mathbf{\Pi}_{\Sigma_h} \nabla\varphi]] \boldsymbol{\beta} \cdot [[v]] \\ &= -a_h(v, \varphi) + \omega^2 \int_{\Omega} v\varphi + S_h(v, \nabla\varphi - \mathbf{\Pi}_{\Sigma_h} \nabla\varphi), \end{aligned}$$

where we have applied sequentially the definition of a_h cf. (21), the fact that $\mathbf{S}_h(v) \in \Sigma_h$, the definitions of \mathbf{S}_h and its associated bilinear form S_h cf. (9) and (17) respectively, and that $[[\nabla\varphi]] = 0$ on any $e \in \mathcal{E}_I$.

Take now $v = u - u_h$ above. We can then check that for any $\psi \in V_h$,

$$\begin{aligned} - \int_{\Omega} (u - u_h)z &= -a_h(u - u_h, \varphi) + \omega^2 \int_{\Omega} (u - u_h)\varphi + S_h(u - u_h, \nabla\varphi - \mathbf{\Pi}_{\Sigma_h} \nabla\varphi) \\ &= -a_h(u - u_h, \varphi - \psi) + \omega^2 \int_{\Omega} (u - u_h)(\varphi - \psi) \\ &\quad + a_h(u_h, \psi) - \omega^2 \int_{\Omega} u_h\psi - a_h(u, \psi) + \omega^2 \int_{\Omega} u\psi + S_h(u - u_h, \nabla\varphi - \mathbf{\Pi}_{\Sigma_h} \nabla\varphi) \\ &= -a_h(u - u_h, \varphi - \psi) + \omega^2 \int_{\Omega} (u - u_h)(\varphi - \psi) \\ &\quad + \mathcal{F}_h(\psi) - a_h(u, \psi) + \omega^2 \int_{\Omega} u\psi + S_h(u - u_h, \nabla\varphi - \mathbf{\Pi}_{\Sigma_h} \nabla\varphi) \\ &= -a_h(u - u_h, \varphi - \psi) + \omega^2 \int_{\Omega} (u - u_h)(\varphi - \psi) + R_h(u, \psi) \\ &\quad + S_h(u - u_h, \nabla\varphi - \mathbf{\Pi}_{\Sigma_h} \nabla\varphi). \end{aligned}$$

The result follows now readily by applying (25). \square

Now we are in position to establish a bound of the second term in (24). Hereafter, we denote by $\|A\|_{X \rightarrow Y}$ the operator norm of a linear mapping $A : X \rightarrow Y$ between two normed spaces X and Y .

Proposition 3.5 Under the same notations defined above, and for all $u \in H^{l+1}(\mathcal{T}_h)$ with $1/2 < l \leq m$,

$$\begin{aligned} \sup_{0 \neq z \in V_h} \frac{1}{\|z\|_h} \left| \int_{\Omega} (u - u_h)z \right| &\leq C_P \|\mathcal{L}_\omega\|_{L^2(\Omega) \rightarrow H^{1+\varepsilon}(\Omega)} \left[((C_{\text{cont}}C_\varepsilon + C_{\varepsilon,S})h^\varepsilon + C_P C_\varepsilon \omega^2 h^{1+\varepsilon}) \|u - u_h\|_h \right. \\ &\quad \left. + C'_{l,S} \left[\sum_{T \in \mathcal{T}_h} h_T^{2l} |\nabla u|_{l,T}^2 \right]^{1/2} \right], \end{aligned} \quad (26)$$

where $C'_{l,S}, C_\varepsilon, C_{\varepsilon,S} > 0$, with $\varepsilon > 1/2$ being as in (4) and $C_P > 0$ the Poincaré-type inequality constant given in (13), all of them independent of \mathcal{T}_h, ω and u .

Proof. Taking $\psi = \Pi_{V_h} \mathcal{L}_\omega z$ in Lemma 3.4 and applying Theorem 3.3 and the Cauchy-Schwarz inequality we derive

$$\begin{aligned} \left| \int_{\Omega} (u - u_h)z \right| &\leq C_{\text{cont}} \|u - u_h\|_h \|\mathcal{L}_\omega z - \Pi_{V_h} \mathcal{L}_\omega z\|_h + \omega^2 \|u - u_h\|_{0,\Omega} \|\mathcal{L}_\omega z - \Pi_{V_h} \mathcal{L}_\omega z\|_{0,\Omega} \\ &\quad + \left| S_h(u_h - u, \mathbf{\Pi}_{\Sigma_h} \nabla \mathcal{L}_\omega z - \nabla \mathcal{L}_\omega z) \right| + \left| S_h(\Pi_{V_h} \mathcal{L}_\omega z, \mathbf{\Pi}_{\Sigma_h} \nabla u - \nabla u) \right|. \end{aligned} \quad (27)$$

Estimate (16) implies

$$\begin{aligned} \|\mathcal{L}_\omega z - \Pi_{V_h} \mathcal{L}_\omega z\|_{0,\Omega} + h \|\mathcal{L}_\omega z - \Pi_{V_h} \mathcal{L}_\omega z\|_h &\leq C_\varepsilon h^{1+\varepsilon} \|\mathcal{L}_\omega z\|_{1+\varepsilon,\Omega} \\ &\leq C_\varepsilon h^{1+\varepsilon} \|\mathcal{L}_\omega\|_{L^2(\Omega) \rightarrow H^{1+\varepsilon}(\Omega)} \|z\|_{0,\Omega}, \end{aligned}$$

which together with Poincaré inequality (13) let us to bound the first two terms of (27).

Regarding the third term, using (25) we deduce

$$\begin{aligned} |S_h(u - u_h, \nabla \mathcal{L}_\omega z - \mathbf{\Pi}_{\Sigma_h} \nabla \mathcal{L}_\omega z)| &\leq C_{\varepsilon,S} \|u - u_h\|_h \left[\sum_{T \in \mathcal{T}_h} h_T^{2\varepsilon} |\nabla \mathcal{L}_\omega z|_{\varepsilon,T}^2 \right]^{1/2} \\ &\leq C_{\varepsilon,S} h^\varepsilon \|u - u_h\|_h \|\mathcal{L}_\omega z\|_{1+\varepsilon,\Omega} \\ &\leq C_{\varepsilon,S} h^\varepsilon \|\mathcal{L}_\omega\|_{L^2(\Omega) \rightarrow H^{1+\varepsilon}(\Omega)} \|u - u_h\|_h \|z\|_{0,\Omega}. \end{aligned}$$

Finally, for the last term in (27) we proceed analogously as before to obtain:

$$\begin{aligned} |(S_h(\Pi_{V_h} \mathcal{L}_\omega z, \mathbf{\Pi}_{\Sigma_h} \nabla u - \nabla u))| &\leq C_{l,S} (\|\Pi_{V_h} \mathcal{L}_\omega z - \mathcal{L}_\omega z\|_h + \|\mathcal{L}_\omega z\|_h) \left[\sum_{T \in \mathcal{T}_h} h_T^{2l} |\nabla u|_{l,T}^2 \right]^{1/2} \\ &\leq C_{l,S} (C_\varepsilon h^\varepsilon + 1) \|\mathcal{L}_\omega z\|_{1+\varepsilon,\Omega} \left[\sum_{T \in \mathcal{T}_h} h_T^{2l} |\nabla u|_{l,T}^2 \right]^{1/2} \\ &\leq C'_{l,S} \|\mathcal{L}_\omega\|_{L^2(\Omega) \rightarrow H^{1+\varepsilon}(\Omega)} \left[\sum_{T \in \mathcal{T}_h} h_T^{2l} |\nabla u|_{l,T}^2 \right]^{1/2} \|z\|_{0,\Omega}, \end{aligned}$$

with $C'_{l,S} := C_{l,S}(C_\varepsilon \text{diam}(\Omega)^\varepsilon + 1)$. The proof is now finished, once we apply Poincaré inequality (13). \square

We are ready to prove the main result of this paper.

Proof of Theorem 3.1. Let u be the exact solution of (1) and suppose u_h is a solution of (20). Next, we take an arbitrary $v \in V_h$ and write

$$\|u_h - u\|_h \leq \|u_h - v\|_h + \|v - u\|_h.$$

By applying (25) and (26) of Proposition 3.5 in (24), we derive the following bound for the first term:

$$(1 - c(\omega, h, \varepsilon)) \|u_h - v\|_h \leq C_2(\omega, \varepsilon) \left[\sum_{T \in \mathcal{T}_h} h_T^{2l} |\nabla u|_{l,T}^2 \right]^{1/2} + c_{\text{coerc}}^{-1} C_{\text{cont}} \|u - v\|_h,$$

where

$$c(\omega, h, \varepsilon) := c_{\text{coer}}^{-1} \omega^2 C_{\text{P}} \|\mathcal{L}\omega\|_{L^2(\Omega) \rightarrow H^{1+\varepsilon}(\Omega)} h^\varepsilon ((C_{\text{cont}} C_\varepsilon + C_{\varepsilon, S}) + C_{\text{P}} C_\varepsilon \omega^2 h), \quad (28)$$

$$C_2(\omega, \varepsilon) := c_{\text{coer}}^{-1} (1 + \omega^2 C_{\text{P}} \|\mathcal{L}\omega\|_{L^2(\Omega) \rightarrow H^{1+\varepsilon}(\Omega)}) C'_{l, S}. \quad (29)$$

By taking h_0 small, say for instance,

$$c(\omega, h_0, \varepsilon) \leq 1/2,$$

and setting $v = \Pi_{V_h} u$, we have that for $h < h_0$,

$$\|u_h - u\|_h \leq C(\omega, \varepsilon) \left[\sum_{T \in \mathcal{T}_h} h_T^{2l} |\nabla u|_{l, T}^2 \right]^{1/2}, \quad (30)$$

where

$$C(\omega, \varepsilon) := 2C_2(\omega, \varepsilon) + (2c_{\text{coerc}}^{-1} C_{\text{cont}} + 1) C_l.$$

Now, the proof of uniqueness solvability of the numerical scheme relies in the fact that the associated homogeneous discrete linear system has only the trivial solution. Indeed, if the exact solution is $u = 0$ and u_h is a solution of the discrete method, then (30) yields

$$\|u_h\|_h \leq 0,$$

and therefore $u_h = 0$ is the only solution of the homogeneous scheme. Thus, we conclude that the LDG scheme always has only one solution, for h small enough.

Finally, the convergence for σ_h follows from standard arguments. Hence, using (19),

$$\begin{aligned} \|\sigma_h - \nabla u\|_{0, \Omega} &\leq \|\nabla_h u_h - \nabla u\|_{0, \Omega} + \|\mathbf{S}_h(u_h) - \mathbf{G}_h(g_D)\|_{0, \Omega} \\ &\leq \|u - u_h\|_h + \|\mathbf{S}_h(u_h - u)\|_{0, \Omega} \\ &\leq C \|u - u_h\|_h, \end{aligned} \quad (31)$$

and we end the proof. \square

Remark 3.6 For the pure Neumann problem, the function $\|u_h\|_h$ (see (12)) is not longer a norm, but a seminorm. This problem can be covered by working instead with $\|u_h\|_h + \|u_h\|_{0, \Omega}$, which becomes again a norm, satisfying in addition the Poincaré inequality. The bilinear form a_h (21) has to be also slightly modified, by adding a L^2 term, to make it elliptic in this norm. The rest of the analysis is essentially the same. We leave this case as a simple exercise for the reader. \square

3.4 The case of complex ω

Let us finish this section analyzing the case of ω being a complex number with positive imaginary part. Problem (1) admits now a unique solution and it is easy to see that the LDG method is stable and convergent via an inf-sup condition.

Let us prove that. First, we write

$$\omega = |\omega| e^{i\theta},$$

with $\theta \in (0, \pi)$. Then for all $0 \neq v \in V_h$ and $\phi \in (0, \pi)$

$$\sup_{0 \neq t \in V_h} \frac{1}{\|t\|_h} \left| a_h(v, t) - \omega^2 \int_{\Omega} vt \right| \geq \frac{1}{\|v\|_h} \text{Re} \left(e^{i\phi} a_h(v, \bar{v}) + e^{i(2\theta + \phi - \pi)} |\omega|^2 \int_{\Omega} |v|^2 \right),$$

simply by taking $t = e^{i\phi} \bar{v}$. Setting

$$\phi := \begin{cases} \pi/2 - 2\theta, & \theta \in (0, \pi/4), \\ 0, & \theta \in [\pi/4, 3\pi/4], \\ 3\pi/2 - 2\theta, & \theta \in (3\pi/4, \pi), \end{cases}$$

and using the coercivity of the bilinear form a_h (cf. Theorem 3.3) and that $\cos(2\theta + \phi - \pi) \geq 0$, we can prove

$$\sup_{0 \neq t \in V_h} \frac{1}{\|t\|_h} \left| a_h(v, t) - \omega^2 \int_{\Omega} vt \right| \geq \frac{\cos \phi}{\|v_h\|_h} a_h(v, \bar{v}) \geq \hat{c}_{\text{coer}}(\theta) \|v\|_h,$$

where

$$\hat{c}_{\text{coer}}(\theta) := \begin{cases} c_{\text{coer}}, & \theta \in [\pi/4, 3\pi/4], \\ |\sin 2\theta| c_{\text{coer}}, & \theta \in (0, \pi/4) \cup (3\pi/4, \pi), \end{cases}$$

with the positive constant c_{coer} given in Theorem 3.3.

Let u_h be a numerical solution of (20). Then, for a given $v \in V_h$ we have

$$\begin{aligned} \hat{c}_{\text{coer}}(\theta) \|u_h - v\|_h &\leq \sup_{0 \neq t \in V_h} \frac{1}{\|t\|_h} \left| a_h(u_h - v, t) - \omega^2 \int_{\Omega} (u_h - v)t \right| \\ &= \sup_{0 \neq t \in V_h} \frac{1}{\|t\|_h} \left| R_h(u, t) + a_h(u - v, t) - \omega^2 \int_{\Omega} (u - v)t \right|. \end{aligned}$$

Hence taking $v = \Pi_{V_h} u$, and using (25), Theorem 3.3 and (16), we easily derive

$$\begin{aligned} \|u - u_h\|_h &\leq \|u - \Pi_{V_h} u\|_h + \|u_h - \Pi_{V_h} u\|_h \\ &\leq (\hat{c}_{\text{coer}}^{-1}(\theta) C_{\text{cont}} + 1) \|u - \Pi_{V_h} u\|_h + \hat{c}_{\text{coer}}^{-1}(\theta) C_{l,S} \left[\sum_{T \in \mathcal{T}_h} h_T^{2l} |\nabla u|_{l,T}^2 \right]^{1/2} \\ &\quad + |\omega|^2 \hat{c}_{\text{coer}}^{-1}(\theta) C_P C_l \left[\sum_{T \in \mathcal{T}_h} h_T^{2l+2} |\nabla u|_{l,T}^2 \right]^{1/2}. \end{aligned} \quad (32)$$

Hence, the stability of the LDG method occurs without assuming any regularity for the adjoint problem and it is not affected by ω itself, but by the argument of ω , i.e., by θ . Notice, however, that $\hat{c}_{\text{coer}}(\theta) \rightarrow 0$ as $\theta \rightarrow 0, \pi$. On the other hand, $|\omega|^2$ does penalize the convergence such as it can be clearly seen in the last term in (32).

4 A posteriori error analysis

The aim of this section is to develop an a posteriori error estimator for the LDG scheme (8). To this end, we first use the auxiliary dual problem (3) to bound the $\|u - u_h\|_{0,\Omega}$. Next, a Helmholtz decomposition is introduced to derive a reliable and efficient a posteriori error estimate. Hereafter, we introduce $\text{curl } v := (-\frac{\partial v}{\partial y}, \frac{\partial v}{\partial x})$ for any $v \in H^1(\Omega)$, and the Sobolev space $H_{\Gamma_D}^1 := \{v \in H^1(\Omega) : v = 0 \text{ on } \Gamma_D\}$.

The main result of the present section is summarized in the next theorem.

Theorem 4.1 *Let $(\sigma, u) \in H(\text{div}, \Omega) \times H^1(\Omega)$ and $(\sigma_h, u_h) \in \Sigma_h \times V_h$ the unique solution of Problems (2) and (8), respectively. Then there exist $C_{\text{rel}}, C_{\text{eff}} > 0$, independent of the meshsize and the wave number, such that*

$$\|u - u_h\|_h^2 + \|\sigma - \sigma_h\|_{0,\Omega}^2 \leq C_{\text{rel}}^2 (1 + \omega^2)^2 \eta^2 := C_{\text{rel}}^2 (1 + \omega^2)^2 \sum_{T \in \mathcal{T}_h} \eta_T^2, \quad (33)$$

where for any $T \in \mathcal{T}_h$ we define

$$\begin{aligned} \eta_T^2 &:= h_T^2 \|f + \omega^2 u_h + \Delta u_h\|_{0,T}^2 + \|\nabla u_h - \sigma_h\|_{0,T}^2 + h_T \|\hat{\sigma} \cdot \nu_T - \nabla u_h \cdot \nu_T\|_{0,\partial T \setminus \Gamma_D}^2 \\ &\quad + \|\alpha^{1/2} [u_h]\|_{0,\partial T \cap \mathcal{E}_I}^2 + \|\alpha^{1/2} (g_D - u_h)\|_{0,\partial T \cap \mathcal{E}_D}^2. \end{aligned} \quad (34)$$

Moreover, for each $T \in \mathcal{T}_h$:

$$\begin{aligned} \eta_T^2 &\leq C_{\text{eff}}^2 (\|\sigma - \sigma_h\|_{0,\mathcal{N}(T)}^2 + \|\nabla u - \nabla_h u_h\|_{0,\mathcal{N}(T)}^2 + \omega^4 h_T^2 \|u - u_h\|_{0,\mathcal{N}(T)}^2 \\ &\quad + \|\alpha^{1/2} [u - u_h]\|_{0,\partial T \cap \mathcal{E}_I}^2 + \|\alpha^{1/2} (g_D - u_h)\|_{0,\partial T \cap \mathcal{E}_D}^2) + h.o.t. \end{aligned} \quad (35)$$

where

$$\mathcal{N}(T) := \bigcup_{\partial T' \cap \partial T \in \mathcal{E}} T',$$

and *h.o.t.* stands for higher order terms.

The proof is presented in the two following subsections.

4.1 Reliability of the estimator

Our first aim is to estimate $\|e_u\|_{0,\Omega}$, where $e_u := u - u_h$ in Ω . For this purpose, we take into account Hypothesis 1.1 and introduce the function $\phi := \mathcal{L}_\omega e_u$, that is,

$$-\Delta \phi - \omega^2 \phi = e_u, \quad \text{in } \Omega \quad \phi|_{\Gamma_D} = 0, \quad \partial_\nu \phi|_{\Gamma_N} = 0. \quad (36)$$

Let Π_0 be the piecewise constant projection from $H^1(\Omega)$ onto $L^2(\Omega)$ defined by

$$(\Pi_0 z)|_T := \begin{cases} \frac{1}{|T|} \int_T z, & \text{if } T \cap \Gamma_D = \emptyset, \\ 0, & \text{otherwise.} \end{cases}$$

By combining the classical results on convergence of the L^2 -orthogonal projection and the local Poincaré inequality on the triangles with a side lying on Γ_D , we can prove

$$\|\psi - \Pi_0 \psi\|_{0,T} \leq C h_T \|\nabla \psi\|_{0,T}, \quad \|\psi - \Pi_0 \psi\|_{0,\partial T} \leq C h_T^{1/2} \|\nabla \psi\|_{0,T}, \quad (37)$$

for all $T \in \mathcal{T}_h$, with $C > 0$ independent of T and ψ . (See [9, Lemma 5.1] for a detailed analysis of this projection).

Lemma 4.2 *Let $z \in H_{\Gamma_D}^1(\Omega)$ and Π_0 the above projection. Then there holds*

$$\sum_{T \in \mathcal{T}_h} \int_{\partial T} \nabla e_u \cdot \nu_T (z - \Pi_0 z) = \sum_{T \in \mathcal{T}_h} \int_{\partial T \setminus \Gamma_D} (\widehat{\sigma} \cdot \nu_T - \nabla u_h \cdot \nu_T) (z - \Pi_0 z) + \omega^2 \int_{\Omega} e_u \Pi_0 z.$$

Proof. Since $[\nabla u] = [\widehat{\sigma}] = 0$ on \mathcal{E}_I , and $z \in H_{\Gamma_D}^1(\Omega)$, it holds

$$\sum_{T \in \mathcal{T}_h} \int_{\partial T} z \nabla u \cdot \nu_T = \int_{\Gamma_N} z g_N = \sum_{T \in \mathcal{T}_h} \int_{\partial T \setminus \Gamma_D} z \widehat{\sigma} \cdot \nu_T.$$

Observe that, by taking $v = 1$ in (5), the following identity holds

$$\int_T f + \omega^2 \int_T u_h + \int_{\partial T} \widehat{\sigma} \cdot \nu_T = 0.$$

Therefore, integrating by parts and taking into account that $\Pi_0 u$ is constant on each triangle,

$$\begin{aligned} \int_{\partial T} \nabla u \cdot \nu_T \Pi_0 z &= \int_T \Delta u \Pi_0 z = \int_T (-f - \omega^2 u) \Pi_0 z \\ &= \int_{\partial T \setminus \Gamma_D} \widehat{\sigma} \cdot \nu_T \Pi_0 z - \omega^2 \int_T (u - u_h) \Pi_0 z. \end{aligned}$$

(We have used also that $\Pi_0 z|_{\Gamma_D} = 0$). The result follows now readily. \square

Lemma 4.3 *Let $z \in H_{\Gamma_D}^1(\Omega)$. Then there holds*

$$\begin{aligned} \sum_{T \in \mathcal{T}_h} \int_T \nabla e_u \cdot \nabla z &= \sum_{T \in \mathcal{T}_h} \int_T (f + \omega^2 u_h + \Delta u_h) (z - \Pi_0 z) \\ &\quad + \sum_{T \in \mathcal{T}_h} \int_{\partial T \setminus \Gamma_D} (\widehat{\sigma} \cdot \nu_T - \nabla u_h \cdot \nu_T) (z - \Pi_0 z) + \omega^2 \int_{\Omega} e_u z. \end{aligned}$$

Proof. We proceed as in Lemma 3.2 in [10] (see also [4] and [5]). Note again that $(\Pi_0 z)|_T$ is constant, and that $z|_{\Gamma_D} = \Pi_0 z|_{\Gamma_D} = 0$. Thus

$$\begin{aligned} \sum_{T \in \mathcal{T}_h} \int_T \nabla e_u \cdot \nabla z &= \sum_{T \in \mathcal{T}_h} \int_T \nabla(u - u_h) \cdot \nabla(z - \Pi_0 z) \\ &= \sum_{T \in \mathcal{T}_h} \left\{ \int_T (f + \omega^2 u_h + \Delta u_h)(z - \Pi_0 z) + \omega^2 \int_T e_u(z - \Pi_0 z) \right. \\ &\quad \left. + \int_{\partial T} \nabla e_u \cdot \boldsymbol{\nu}_T(z - \Pi_0 z) \right\}. \end{aligned}$$

The proof is finished once Lemma 4.2 is applied to bound the last term in equation above. \square

Proposition 4.4 *There exists $C > 0$, independent of the meshsize h and the wave number ω , such that*

$$\|e_u\|_{0,\Omega}^2 \leq C^2 \hat{\eta}^2 := C^2 \sum_{T \in \mathcal{T}_h} \hat{\eta}_T^2,$$

where, for each $T \in \mathcal{T}_h$, we define

$$\begin{aligned} \hat{\eta}_T^2 &:= h_T^2 \|f + \omega^2 u_h + \Delta u_h\|_{0,T}^2 + h_T \|\hat{\boldsymbol{\sigma}} \cdot \boldsymbol{\nu}_T - \nabla u_h \cdot \boldsymbol{\nu}_T\|_{0,\partial T \setminus \Gamma_D}^2 \\ &\quad + \|\alpha^{1/2} \llbracket u_h \rrbracket\|_{0,\partial T \cap \mathcal{E}_I}^2 + \|\alpha^{1/2} (g_D - u_h)\|_{0,\partial T \cap \mathcal{E}_D}^2. \end{aligned}$$

Proof. Take $\phi = \mathcal{L}_\omega e_u \in H_{\Gamma_D}^1(\Omega) \cap H^{1+\varepsilon}(\Omega)$. Then, integrating by parts and making use of Lemma 4.3 we can obtain

$$\begin{aligned} \|e_u\|_{0,\Omega}^2 &= \sum_{T \in \mathcal{T}_h} \int_T e_u (-\Delta \phi - \omega^2 \phi) = \sum_{T \in \mathcal{T}_h} \left\{ \int_T \nabla e_u \cdot \nabla \phi - \omega^2 \int_T \phi e_u - \int_{\partial T \setminus \Gamma_N} e_u \nabla \phi \cdot \boldsymbol{\nu}_T \right\} \\ &= \sum_{T \in \mathcal{T}_h} \left\{ \int_T (f + \omega^2 u_h + \Delta u_h)(\phi - \Pi_0 \phi) + \int_{\partial T \setminus \Gamma_D} (\hat{\boldsymbol{\sigma}} \cdot \boldsymbol{\nu}_T - \nabla u_h \cdot \boldsymbol{\nu}_T)(\phi - \Pi_0 \phi) \right. \\ &\quad \left. - \int_{\partial T \setminus \Gamma} \nabla \phi \cdot \llbracket u_h \rrbracket \right\} - \int_{\mathcal{E}_D} \nabla \phi \cdot \llbracket g_D - u_h \rrbracket. \end{aligned} \quad (38)$$

where in the last step we have applied Lemma 4.2, with $z = \phi$, used the relation $-\Delta u - \omega^2 u = f$ in Ω and that $\llbracket \nabla \phi \rrbracket = 0$, on any $e \in \mathcal{E}_I \cup \mathcal{E}_N$ and $\llbracket u \rrbracket = 0$, on any $e \in \mathcal{E}_I$.

Note (cf. [21]) that

$$\|w\|_{0,\partial T} \leq C_s h_T^{s-1/2} \|w\|_{s,T} \quad \forall w \in H^s(T),$$

with $C_s > 0$ depending only on $s > 1/2$. Then, using this bound, as well as the definition of α , we can easily check

$$\left| \int_{\partial T} \nabla \phi \cdot \llbracket u_h \rrbracket \right| \leq \|\alpha^{-1/2} \nabla \phi\|_{0,\partial T} \|\alpha^{1/2} \llbracket u_h \rrbracket\|_{0,\partial T} \leq C' \|\phi\|_{1+\varepsilon,T} \|\alpha^{1/2} \llbracket u_h \rrbracket\|_{0,\partial T}.$$

Applying first this inequality and (37) to the first two terms in (38) and next the Cauchy-Schwarz inequality, we get

$$\|e_u\|_{0,\Omega}^2 \leq C \sum_{T \in \mathcal{T}_h} \hat{\eta}_T \|\phi\|_{1+\varepsilon,T} \leq C \left[\sum_{T \in \mathcal{T}_h} \hat{\eta}_T^2 \right]^{1/2} \|\phi\|_{1+\varepsilon,\Omega} \leq C \|\mathcal{L}_\omega\|_{L^2(\Omega) \rightarrow H^{1+\varepsilon}(\Omega)} \left[\sum_{T \in \mathcal{T}_h} \hat{\eta}_T^2 \right]^{1/2} \|e_u\|_{0,\Omega},$$

where we have applied in the last step Hypothesis 1.1. The proof is now completed. \square

To derive a a posteriori error estimator for $\|u - u_h\|_h$ we will make use of the following Helmholtz decomposition.

Lemma 4.5 *There exist $\psi \in H_{\Gamma_D}^1(\Omega)$ and $\chi \in H^1(\Omega)$ with $\text{curl } \chi \cdot \boldsymbol{\nu} = 0$ on Γ_N , such that*

$$\nabla_h e_u = \nabla \psi + \text{curl } \chi.$$

Furthermore, there holds

$$\|\nabla \psi\|_{0,\Omega}^2 + \|\text{curl } \chi\|_{0,\Omega}^2 = \|\nabla_h(u - u_h)\|_{0,\Omega}^2.$$

Proof. It is consequence of Theorem I.3.1 in [22]. We refer also to Lemma 3.1 in [10] for more details. \square

Lemma 4.6 *Let $\chi \in H^1(\Omega)$ the function from Lemma 4.5. Then there exists $c > 0$, independent of h and ω , such that*

$$\begin{aligned} \sum_{T \in \mathcal{T}_h} \int_T \nabla e_u \cdot \text{curl } \chi &\leq c \|\text{curl } \chi\|_{0,\Omega} \|e_u\|_h \\ &= c \left(\|\alpha^{1/2} \llbracket u_h \rrbracket\|_{0,\mathcal{E}_I}^2 + \|\alpha^{1/2} (g_D - u_h)\|_{0,\mathcal{E}_D}^2 \right)^{1/2} \|\text{curl } \chi\|_{0,\Omega} \quad \forall u \in H^1(\mathcal{T}_h). \end{aligned}$$

Proof. See Lemma 4.4 in [4]. \square

We are ready to derive the a posteriori estimate for $\|u - u_h\|_h$ and $\|\boldsymbol{\sigma} - \boldsymbol{\sigma}_h\|_{0,\Omega}$.

Proof of (33) of Theorem 4.1. Notice that since

$$\|\boldsymbol{\sigma} - \boldsymbol{\sigma}_h\|_{0,\Omega} \leq C \|u - u_h\|_h,$$

(see (31)), it suffices to bound $\|u - u_h\|_h$.

We then proceed as in Theorem 3.2 in [10] (see also [5]). Since $\llbracket u \rrbracket = 0$ in \mathcal{E}_I and g_D in \mathcal{E}_D , we deduce

$$\|u - u_h\|_h^2 = \|e_u\|_h^2 = \|\nabla_h e_u\|_{0,\Omega}^2 + \|\alpha^{1/2} \llbracket u_h \rrbracket\|_{0,\mathcal{E}_I}^2 + \|\alpha^{1/2} (g_D - u_h)\|_{0,\mathcal{E}_D}^2. \quad (39)$$

Besides,

$$\|\nabla_h e_u\|_{0,\Omega}^2 = \sum_{T \in \mathcal{T}_h} \left\{ \int_T \nabla e_u \cdot \nabla \psi + \int_T \nabla e_u \cdot \text{curl } \chi \right\}. \quad (40)$$

The first term can be bounded as follows:

$$\begin{aligned} \sum_{T \in \mathcal{T}_h} \int_T \nabla e_u \cdot \nabla \psi &= \sum_{T \in \mathcal{T}_h} \left\{ \int_T (f + \omega^2 u_h + \Delta u_h) (\psi - \Pi_0 \psi) + \int_{\partial T \setminus \Gamma_D} (\widehat{\boldsymbol{\sigma}} \cdot \boldsymbol{\nu}_T - \nabla u_h \cdot \boldsymbol{\nu}_T) (\psi - \Pi_0 \psi) \right\} \\ &\quad + \omega^2 \|e_u\|_{0,\Omega} \|\psi\|_{0,\Omega} \\ &\leq C \left(\left[\sum_{T \in \mathcal{T}_h} \left\{ (h_T \|f + \omega^2 u_h + \Delta u_h\|_{0,T} + h_T^{1/2} \|\widehat{\boldsymbol{\sigma}} \cdot \boldsymbol{\nu}_T - \nabla u_h \cdot \boldsymbol{\nu}_T\|_{0,\partial T}) \|\nabla \psi\|_{0,T} \right\} \right]^2 \right. \\ &\quad \left. + C_P^2 \omega^4 \|e_u\|_{0,\Omega}^2 \|\nabla \psi\|_{0,\Omega}^2 \right)^{1/2} \\ &\leq C' (1 + \omega^2) \left[\sum_{T \in \mathcal{T}_h} \eta_T^2 \right]^{1/2} \|\nabla \psi\|_{0,\Omega}, \end{aligned}$$

where we have applied sequentially Lemmas 4.3 and 4.5, estimate (37), Poincaré inequality (13), the Cauchy-Schwarz inequality and, finally, to bound the term $\|e_u\|_{0,\Omega}$, Proposition 4.4.

Using this result, and Lemma 4.6 in (40) we derive

$$\begin{aligned} \|\nabla_h e_u\|_{0,\Omega}^2 &\leq C(1 + \omega^2) \left[\sum_{T \in \mathcal{T}_h} \eta_T^2 \right]^{1/2} (\|\nabla \psi\|_{0,\Omega}^2 + \|\text{curl } \chi\|_{0,\Omega}^2)^{1/2} \\ &= C(1 + \omega^2) \left[\sum_{T \in \mathcal{T}_h} \eta_T^2 \right]^{1/2} \|\nabla_h e_u\|_{0,\Omega}. \end{aligned} \quad (41)$$

Inserting (41) in (39), the result is proven. \square .

4.2 Quasi-efficiency of the estimator

In this subsection we prove the quasi-efficiency of the estimator (cf. (35)). For simplicity, we assume that each element of $\{\mathcal{T}_h\}_{h>0}$ has not hanging node.

We begin with some notations and preliminary results. For each $T \in \mathcal{T}_h$ and e an edge of T , we will denote in this section only by $\mathbb{P}_m(T)$ and $\mathbb{P}_m(e)$ the spaces of polynomials on T and e respectively of degree m . On the other hand, we denote by ψ_T and ψ_e the standard triangle-bubble and edge-bubble functions, respectively. In particular, ψ_T satisfies

$$\psi_T \in \mathbb{P}_3(T), \quad \text{supp}(\psi_T) \subseteq T, \quad \text{with } 0 \leq \psi_T \leq 1 \quad \text{and} \quad \psi_T|_{\partial T} = 0.$$

Similarly,

$$\psi_e|_T \in \mathbb{P}_2(T), \quad \text{supp}(\psi_e) \subseteq \cup\{T' \in \mathcal{T}_h : e \subset \partial T'\}, \quad \text{with } 0 \leq \psi_e \leq 1 \quad \text{and} \quad \psi_e|_{\partial T \setminus e} = 0.$$

We also recall from [39] that, given $k \in \mathbb{N} \cup \{0\}$, there exists an extension operator $L : C(e) \rightarrow C(T)$ that satisfies

$$Lp \in \mathbb{P}_m(T), \quad Lp|_e = p, \quad \forall p \in \mathbb{P}_m(e).$$

Additional properties of ψ_T , ψ_e , and L are listed here cf. [39, Lemma 1.3]: There exist $c_1, c_2, c_3, c_4 > 0$ so that

$$\|\psi_T q\|_{0,T}^2 \leq \|q\|_{0,T}^2 \leq c_1 \|\psi_T^{1/2} q\|_{0,T}^2 \quad \forall q \in \mathbb{P}_m(T), \quad (42)$$

$$\|\psi_e p\|_{0,e}^2 \leq \|p\|_{0,e}^2 \leq c_2 \|\psi_e^{1/2} p\|_{0,e}^2 \quad \forall p \in \mathbb{P}_m(e), \quad (43)$$

$$c_4 h_e \|p\|_{0,e}^2 \leq \|\psi_e^{1/2} Lp\|_{0,T}^2 \leq c_3 h_e \|p\|_{0,e}^2 \quad \forall p \in \mathbb{P}_m(e). \quad (44)$$

Our aim now is to estimate these five terms which define the error indicator η_T^2 cf. (34). Observe that we can bound three of them straightforwardly, namely

$$\|\nabla u_h - \sigma_h\|_{0,T} \leq \|\sigma - \sigma_h\|_{0,T} + \|\nabla e_u\|_{0,T} \quad \forall T \in \mathcal{T}_h \quad (45)$$

$$\|\alpha^{1/2} [u_h]\|_{0,e} = \|\alpha^{1/2} [e_u]\|_{0,e} \quad \forall e \in \mathcal{E}_I, \quad (46)$$

$$\|\alpha^{1/2} (g_D - u_h)\|_{0,e} = \|\alpha^{1/2} (u - u_h)\|_{0,e} \quad \forall e \in \mathcal{E}_D, \quad (47)$$

where as usual $e_u = u - u_h$.

From here on, we introduce $f_h = \Pi_{V_h} f$ so that $\|f - f_h\|_{0,T}$ goes to zero with, at least, the same rate as $\|e_u\|_h$ as the mesh is refined.

Lemma 4.7 *There exists $C > 0$, independent of the mesh size and ω , such that for any $T \in \mathcal{T}_h$*

$$h_T^2 \|f + \omega^2 u_h + \Delta u_h\|_{0,T}^2 \leq C (\|\nabla e_u\|_{0,T}^2 + \omega^4 h_T^2 \|e_u\|_{0,T}^2 + h_T^2 \|f - f_h\|_{0,T}^2). \quad (48)$$

Proof. Let $v_h := f_h + \omega^2 u_h + \Delta u_h$, and $v_b := \psi_T v_h$. Then

$$\begin{aligned} c_1^{-1} \|v_h\|_{0,T}^2 &\leq \|\psi_T^{1/2} v_h\|_{0,T}^2 = \int_T (v_h + f) v_b - \int_T f v_b = - \int_T \Delta e_u v_b - \omega^2 \int_T e_u v_b + \int_T (f_h - f) v_b \\ &= \int_T \nabla e_u \cdot \nabla v_b - \omega^2 \int_T e_u v_b + \int_T (f_h - f) v_b. \end{aligned}$$

(Note that $v_b|_{\partial T} = 0$). The inverse inequality

$$\|\nabla v_b\|_{0,T} \leq Ch_T^{-1} \|v_b\|_{0,T} \leq Ch_T^{-1} \|v_h\|_{0,T}^2 \quad (49)$$

yields now

$$\|v_h\|_{0,T}^2 \leq C (\omega^2 \|e_u\|_{0,T} + h_T^{-1} \|\nabla e_u\|_{0,T} + \|f - f_h\|_{0,T}) \|v_h\|_{0,T}.$$

The proof is finished by noting now

$$\|f + \omega^2 u_h + \Delta u\|_{0,T}^2 \leq 2\|f - f_h\|_{0,T}^2 + 2\|v_h\|_{0,T}^2 \leq C [\omega^4 \|e_u\|_{0,T}^2 + h_T^{-2} \|\nabla e_u\|_{0,T}^2 + \|f - f_h\|_{0,T}^2].$$

□

Lemma 4.8 *Let $e \in \mathcal{E}_I$, and let $T', T \in \mathcal{T}_h$ so that $T \cap T' = e$. Then, there exists $C > 0$, independent of the mesh size and ω , such that*

$$\begin{aligned} h_e \|\widehat{\boldsymbol{\sigma}} \cdot \boldsymbol{\nu}_T - \nabla u_h \cdot \boldsymbol{\nu}_T\|_{0,e}^2 &\leq C_3 \left(\|\alpha^{1/2} [u - u_h]\|_{0,e}^2 + \|\nabla u - \nabla_h u_h\|_{0,\mathcal{N}(T)}^2 + \|\boldsymbol{\sigma} - \boldsymbol{\sigma}_h\|_{0,\mathcal{N}(T)}^2 \right) \\ &\quad + \omega^4 \max\{h_T, h_{T'}\}^2 \|u - u_h\|_{0,\mathcal{N}(T)}^2 + \max\{h_T, h_{T'}\}^2 \|f - f_h\|_{0,\mathcal{N}(T)}^2. \end{aligned}$$

Proof. It can be easily checked that

$$\|\widehat{\boldsymbol{\sigma}} \cdot \boldsymbol{\nu}_T - \nabla u_h \cdot \boldsymbol{\nu}_T\|_{0,e} \leq C \left\{ \|\llbracket \boldsymbol{\sigma}_h \rrbracket\|_{0,e} + \|\alpha^{1/2} [u_h]\|_{0,e} + \|\boldsymbol{\sigma}_h \cdot \boldsymbol{\nu}_T - \nabla u_h \cdot \boldsymbol{\nu}_T\|_{0,e} \right\}. \quad (50)$$

Clearly, it only remains to bound the first and third term in the inequality above. For the third term, we denote for the sake of a simpler notation

$$\lambda_h := \boldsymbol{\sigma}_h \cdot \boldsymbol{\nu}_T - \nabla u_h \cdot \boldsymbol{\nu}_T.$$

Then, using the property (43) and integrating by parts, we have

$$c_2^{-1} \|\lambda_h\|_{0,e}^2 \leq \|\psi_e^{1/2} \lambda_h\|_{0,e}^2 = \int_T \operatorname{div}(\boldsymbol{\sigma}_h - \nabla u_h)(L\lambda_h) \psi_e + \int_T (\boldsymbol{\sigma}_h - \nabla u_h) \cdot \nabla(\psi_e L\lambda_h).$$

The Cauchy-Schwarz inequality, inverse inequality (49) and (44) yield

$$\begin{aligned} \|\lambda_h\|_{0,e}^2 &\leq C \left\{ h_T^{1/2} \|\operatorname{div}(\boldsymbol{\sigma}_h - \nabla u_h)\|_{0,T} + h_T^{-1/2} \|\boldsymbol{\sigma}_h - \nabla u_h\|_{0,T} \right\} \|\lambda_h\|_{0,e} \\ &\leq C (C_{\text{ineq}} + 1) h_T^{-1/2} \|\boldsymbol{\sigma}_h - \nabla u_h\|_{0,T} \|\lambda_h\|_{0,e}, \end{aligned}$$

where in the last step we have also used cf. [33, Corollary 1]

$$\|\operatorname{div}(\boldsymbol{\tau})\|_{0,T} \leq C_{\text{ineq}} h_T^{-1} \|\boldsymbol{\tau}\|_{0,T}, \quad \forall T \in \mathcal{T}_h \quad \forall \boldsymbol{\tau} \in \boldsymbol{\Sigma}_h, \quad (51)$$

with $C_{\text{ineq}} > 0$ is independent of the mesh size. Regarding the first term $\|\llbracket \boldsymbol{\sigma}_h \rrbracket\|_{0,e}$ in (50) and denoting $w_h := \llbracket \boldsymbol{\sigma}_h \rrbracket \in \mathbb{P}_m(e)$, we deduce

$$\begin{aligned} c_2^{-1} \|w_h\|_{L^2(e)}^2 &\leq \|\psi_e^{1/2} w_h\|_{L^2(e)}^2 = \int_e \psi_e L w_h \llbracket \boldsymbol{\sigma}_h - \boldsymbol{\sigma} \rrbracket \\ &= \int_{T \cup T'} \operatorname{div}(\boldsymbol{\sigma}_h - \boldsymbol{\sigma}) \psi_e L w_h + \int_{T \cup T'} (\boldsymbol{\sigma}_h - \boldsymbol{\sigma}) \cdot \nabla(\psi_e L w_h) \\ &= \int_{T \cup T'} \operatorname{div}(\boldsymbol{\sigma}_h - \nabla_h u_h) \psi_e L w_h + \int_{T \cup T'} (\Delta_h u_h + \omega^2 u_h + f) \psi_e L w_h \\ &\quad + \omega^2 \int_{T \cup T'} (u - u_h) \psi_e L w_h + \int_{T \cup T'} (\boldsymbol{\sigma}_h - \boldsymbol{\sigma}) \cdot \nabla(\psi_e L w_h). \end{aligned}$$

Next, we bound each of the four integrals per element, applying Cauchy-Schwarz and some properties such as inverse inequality, the ones given in (42)-(44), and/or (51). For example, for the element T , we derive

$$\begin{aligned} \int_T \operatorname{div}(\boldsymbol{\sigma}_h - \nabla_h u_h) \psi_e L w_h &\leq c \frac{h_e^{1/2}}{h_T} \|\boldsymbol{\sigma}_h - \nabla_h u_h\|_{0,T} \|w_h\|_{0,e}, \\ \int_T (\Delta_h u_h + \omega^2 u_h + f) \psi_e L w_h &\leq c h_e^{1/2} \|\Delta_h u_h + \omega^2 u_h + f\|_{0,T} \|w_h\|_{0,e}, \\ \int_T (u - u_h) \psi_e L w_h &\leq c h_e^{1/2} \|u - u_h\|_{0,T} \|w_h\|_{0,e}, \end{aligned}$$

and

$$\begin{aligned} \int_T (\boldsymbol{\sigma}_h - \boldsymbol{\sigma}) \cdot \nabla(\psi_e L w_h) &\leq c \frac{h_e^{1/2}}{h_T} \left(\|\boldsymbol{\sigma}_h - \nabla_h u_h\|_{0,T} + \|\nabla u - \nabla_h u_h\|_{0,T} \right. \\ &\quad \left. + \omega^2 h_T \|u - u_h\|_{0,T} + h_T \|f - f_h\|_{0,T} \right) \|w_h\|_{0,e}. \end{aligned}$$

The result is obtained after we summing up the corresponding estimates for T and T' , and applying Lemma 4.7, to bound $\|\Delta_h u_h + \omega^2 u_h + f\|_{0,T}$. We omit further details. \square

5 Numerical examples

In this Section we show the performance of the method with the $\mathbb{P}_1 - [\mathbb{P}_1]^2$ approximation. The code has been written in MATLAB and run in a *Pentium Xeon computer with dual processor*. In what follows, N stands for the total number of degrees of freedom (unknowns) of (8). Hereafter, the individual and total errors are denoted as follows

$$\begin{aligned} e_h(u) &:= \|u - u_h\|_h, & e(\boldsymbol{\sigma}) &:= \|\boldsymbol{\sigma} - \boldsymbol{\sigma}_h\|_{0,\Omega}, \\ e_0(u) &:= \|u - u_h\|_{0,\Omega}, & e &:= \left(e_h(u)^2 + e_0(\boldsymbol{\sigma})^2 \right)^{1/2}, \end{aligned}$$

where $(\boldsymbol{\sigma}, u) \in [L^2(\Omega)]^2 \times H^1(\Omega)$ and $(\boldsymbol{\sigma}_h, u_h) \in \boldsymbol{\Sigma}_h \times V_h$ are the unique solutions of the continuous and discrete formulations, (2) and (8), respectively. In addition, if e and \tilde{e} stand for the errors at two consecutive triangulations with N and \tilde{N} degrees of freedom, respectively, then the experimental rate of convergence is given by $r := -2 \frac{\log(e/\tilde{e})}{\log(N/\tilde{N})}$. The definitions of $r_h(u)$, $r_0(\boldsymbol{\sigma})$, and $r_0(u)$ are given in analogous way. Finally, by e/η we measure the effectivity index.

We now specify the data of the three examples to be presented here. We take Ω as either the square $]0, 1[^2$ (for Example 1) or the L-shaped domains $] -1, 1[^2 \setminus [0, 1]^2$ for Example 2 and $] -1, 1[^2 \setminus [0, 1] \times [-1, 0]$ for Example 3. For Example 2 we define $\bar{\Gamma}_D := \{-1\} \times [-1, 1] \cup \{1\} \times [-1, 0] \cup \{0\} \times [0, 1]$, and we consider $\bar{\Gamma}_D := \{0\} \times [-1, 0] \cup [0, 1] \times \{0\}$ for Example 3. In all these examples, the data f , g_D and/or g_N are chosen so that the exact solution u is the one shown in Table 5.1. We emphasize that the solution u of Example 1 is smooth, while the one of Example 3 (given in polar coordinates) lives in $H^{1+2/3}(\Omega)$, since their derivatives are singular at $(0, 0)$. This implies that $\text{div}(\boldsymbol{\sigma}) \in H^{2/3}(\Omega)$ only, which, according to Theorem 3.1, yields $2/3$ as the expected rate of convergence for the uniform refinement.

Table 5.1. Summary of data for the three examples.

EXAMPLE	DOMAIN Ω	B.C.	ω	SOLUTION u
1	SQUARE	DIRICHLET	1.0	$\sin(\pi x_1) \sin(\pi x_2)$
			4.0	
			4.44	
			4.5	
			5.0	
2	L-SHAPED	MIXED	1.0	$\frac{1}{1.1 - x_1}$
			10.0	
			15.0	
3	L-SHAPED	MIXED	1.0	$r^{2/3} \sin\left(\frac{2}{3}\theta\right)$
			10.0	
			15.0	

The aim of the numerical experiments for Example 1 is to show the robustness of the scheme for different values of the wave number ω when using uniform refinements. Specifically, Tables 5.2 and 5.6 contain the results obtained for $\omega \in \{1, 5\}$, for which ω^2 is far from the first eigenvalue of the problem: $2\pi^2$, while in Tables 5.3-5.5 are shown the results for $\omega \in \{4, 4.44, 4.5\}$, such that ω^2 is closer to $2\pi^2$. In all the cases we observe that the $e_h(u)$ and $e(\boldsymbol{\sigma})$ behave as $\mathcal{O}(h)$, as expected, while the L^2 - error norm of u ($e_0(u)$) converges at a rate of order $\mathcal{O}(h^2)$, which is expected too, but have not been proved here. We remark, since $\omega \in \{4.44, 4.5\}$ is very close to $\sqrt{2}\pi$, the method requires smaller mesh size to behave well, in agreement with the theory (see Tables 5.4 and 5.5). In addition, with the purpose of showing the robustness of the scheme for moderately large value of wave number, we summarize in Tables 5.7 and 5.8 the individual and global errors (including the L^2 - error norm $e_0(u)$) and the effectivity index e/η obtained for $\omega \in \{10, 15\}$, considering Example 1. In both two cases, the choice for ω requires a smaller mesh size to get an appropriate approximation of the exact solution, which are in agreement with the theory. Moreover, the rate of convergence of $e_h(u)$ and $e(\boldsymbol{\sigma})$ is the expected: $\mathcal{O}(h)$. We remark that the

$\mathcal{O}(h^2)$ behavior of $e_0(u)$ using uniform refinement for all examples and choices of ω considered in this work has not been proved here, but we think that it should be derived by a standard duality argument. Furthermore, in order to describe the behavior of the estimator for different values of the wave number ω , in Tables 5.2-5.8 we have included a column with the effectivity indexes. We note that in all cases these indexes remain constants, which is in accordance with the reliability and local efficiency proved here.

Since we have developed an a posteriori error estimator η in Theorem 4.1, we use it to develop an adaptive procedure in order to improve the quality of the initial approximation by refining the zones of $\bar{\Omega}$ where the (local) estimator dominates over (part of) the rest. On the other hand, it is well known that in order to avoid the *pollution effect* we should start with a *coarse* mesh satisfying $\omega h < 1$. To the aim of comparing the adaptive and uniform strategies, we consider the following algorithm, which we called *hybrid adaptive* algorithm:

1. Start with a coarse mesh \mathcal{T}_h .
2. Perform uniform refinements to \mathcal{T}_h until the resulting mesh satisfies $\omega h < 1$. Define this mesh as the new \mathcal{T}_h and go to next step.
3. Solve the Galerkin scheme (8) for the current mesh \mathcal{T}_h .
4. Compute η_T for each triangle $T \in \mathcal{T}_h$.
5. Consider stopping criterion and decide to finish or go to the next step.
6. Use *newest vertex bisection* procedure to refine each element $T' \in \mathcal{T}_h$ such that

$$\eta_{T'} \geq \frac{1}{4} \max\{\eta_T : T \in \mathcal{T}_h\}.$$

7. Define the resulting mesh as the new \mathcal{T}_h and go to step 3.

In practice, we should start with a *suitable* coarse mesh \mathcal{T}_h , satisfying $\omega h < 1$, and go to step 3 in the proposed adaptive algorithm. However, we perform the described algorithm in order to compute the errors and effectivity indexes from a coarsest mesh not verifying the condition on ωh a priori and compared them with results obtained by the adaptive refinement.

We apply this algorithm to Examples 2 and 3. Respect to Example 2, it is not difficult to check that its exact solution has a singularity on the line $x_1 = 1.1$, which at the discrete level results in a numerical singularity on the edge $\{1\} \times [-1, 0]$. In Tables 5.9-5.11 we resume the behavior of the individual and total errors, as well as the index of efficiency, after performing uniform refinement for different values of the wave number ω . In all the cases we observe that the method converges with the optimal rate, and the effectivity index remains bounded. Tables 5.15-5.17 contain the respective output when the proposed adaptive algorithm is applied. In this case, we observe that the method also converges at the same optimal rate, but it is able to detect the numerical singularity in the neighborhood of $\{1\} \times [-1, 0]$, which yields to a boundary layer close to the referred part of $\partial\Omega$. This is better described in Figures 5.1-5.3, where a comparison between the total error obtained performing uniform and adaptive refinements is shown, for $\omega \in \{1, 10, 15\}$. Thanks to the numerical singularity, the adaptive procedure is focused on the large error region and then it improves the quality of the approximation. Some intermediate adapted meshes for each value of ω considered here, are included in Figures 5.7-5.9, where the corresponding boundary layer is recognized and localized.

Now, concerning Example 3, we point out that the gradient of the exact solution is singular at the origin $(0, 0)$, so the expected rate of convergence of the method is of order $\mathcal{O}(h^{2/3})$, for moderate values of the wave number. This is confirmed when performing uniform refinements and can be noticed in Tables 5.12-5.14, where, in addition, the index of efficiency is bounded in all cases. As in the previous example, the adaptive refinement is able to detect the singularity region, and we observe that the optimal rate of convergence is achieved, for different values of ω (cf. Tables 5.18-5.20). Again, in all these cases, the effective index remains bounded. Figures 5.4-5.6 shows the improvement of the quality of the approximation when using adaptivity, for all the values of ω we considered. Some adapted meshes for the wave numbers we set here, are displayed in Figures 5.10-5.12, which exhibit the localization of the

singularity. In addition, it is important to mention that this example behaves as predicted by our theory, despite the fact that it does not rely in it: the geometric condition on the mixed boundary $\partial\Omega$ is not satisfied in the present case so we can not ensure that the adjoint problem has a smooth enough solution (cf. Grisvard [25]). This example gives us, therefore, numerical evidence to conjecture that our results could be proved without using that geometric assumption.

Conclusions and final comments

Summarizing, the numerical results presented here underline the reliability and efficiency of the a posteriori error estimator η , and strongly show that the associated hybrid adaptive algorithms are much more suitable than a uniform discretization procedure when solving problems with non-smooth solutions. We notice that in all the examples we considered, the effectivity index does not behave as the current analysis predicts: $\mathcal{O}(\omega^2)$. This gives us some numerical evidence that the behavior of this index could be overestimated and could be the subject of future research.

Table 5.2. Example 1: uniform refinement with $\omega = 1.0$

N	$e(u)$	$r(u)$	$e(\sigma)$	$r(\sigma)$	e	r	$e_0(u)$	r_0	e/η
36	1.667e+00	—	1.119e+00	—	2.008e+00	—	1.629e-01	—	0.1721
144	9.355e-01	0.8337	4.822e-01	1.2146	1.052e+00	0.9320	5.229e-02	1.6394	0.1721
576	4.863e-01	0.9438	2.803e-01	0.7829	5.613e-01	0.9069	1.552e-02	1.7524	0.1813
2304	2.441e-01	0.9944	1.585e-01	0.8225	2.910e-01	0.9476	4.304e-03	1.8505	0.1912
9216	1.222e-01	0.9983	8.318e-02	0.9298	1.478e-01	0.9773	1.121e-03	1.9414	0.1960
36864	6.117e-02	0.9982	4.237e-02	0.9734	7.441e-02	0.9903	2.846e-04	1.9772	0.1981
147456	3.061e-02	0.9988	2.134e-02	0.9891	3.732e-02	0.9956	7.162e-05	1.9906	0.1990

Table 5.3. Example 1: uniform refinement with $\omega = 4.0$

N	$e(u)$	$r(u)$	$e(\sigma)$	$r(\sigma)$	e	r	$e_0(u)$	r_0	e/η
36	2.731e+01	—	1.797e+01	—	3.269e+01	—	4.623e+00	—	0.3164
144	9.569e-01	4.8348	6.021e-01	4.8993	1.131e+00	4.8537	1.085e-01	5.4135	0.3164
576	5.073e-01	0.9155	3.236e-01	0.8958	6.017e-01	0.9099	4.569e-02	1.2475	0.2304
2304	2.496e-01	1.0230	1.668e-01	0.9566	3.002e-01	1.0032	1.458e-02	1.6484	0.2205
9216	1.231e-01	1.0203	8.438e-02	0.9828	1.492e-01	1.0085	3.975e-03	1.8743	0.2069
36864	6.129e-02	1.0057	4.252e-02	0.9887	7.460e-02	1.0002	1.025e-03	1.9554	0.2012
147456	3.063e-02	1.0009	2.136e-02	0.9931	3.734e-02	0.9983	2.593e-04	1.9829	0.1998

Table 5.4. Example 1: uniform refinement with $\omega = 4.44$

N	$e(u)$	$r(u)$	$e(\sigma)$	$r(\sigma)$	e	r	$e_0(u)$	r_0	e/η
36	2.250e+00	—	2.244e+00	—	3.177e+00	—	5.023e-01	—	43.1922
144	2.164e+00	0.0562	2.161e+00	0.0545	3.058e+00	0.0553	4.863e-01	0.0469	43.1922
576	2.077e+00	0.0589	2.074e+00	0.0591	2.935e+00	0.0590	4.668e-01	0.0590	18.0626
2304	1.803e+00	0.2045	1.800e+00	0.2046	2.547e+00	0.2046	4.050e-01	0.2048	14.7562
9216	1.188e+00	0.6017	1.185e+00	0.6023	1.678e+00	0.6020	2.667e-01	0.6029	8.9778
36864	5.068e-01	1.2290	5.049e-01	1.2313	7.154e-01	1.2301	1.134e-01	1.2336	4.8120
147456	1.562e-01	1.6983	1.546e-01	1.7075	2.197e-01	1.7029	3.451e-02	1.7164	2.4737

Table 5.5. Example 1: uniform refinement with $\omega = 4.5$

N	$e(u)$	$r(u)$	$e(\sigma)$	$r(\sigma)$	e	r	$e_0(u)$	r_0	e/η
36	1.944e+00	—	2.046e+00	—	2.822e+00	—	4.429e-01	—	2.2210
144	5.152e+00	—	5.175e+00	—	7.302e+00	—	1.159e+00	—	2.2210
576	5.368e+00	—	5.356e+00	—	7.583e+00	—	1.187e+00	—	0.9030
2304	6.627e-01	3.0180	6.366e-01	3.0727	9.190e-01	3.0447	1.359e-01	3.1262	0.7514
9216	1.843e-01	1.8462	1.613e-01	1.9805	2.449e-01	1.9075	3.040e-02	2.1607	0.4839
36864	6.994e-02	1.3981	5.430e-02	1.5709	8.854e-02	1.4680	7.466e-03	2.0257	0.3090
147456	3.176e-02	1.1387	2.297e-02	1.2412	3.920e-02	1.1756	1.866e-03	2.0004	0.2333

Table 5.6. Example 1: uniform refinement with $\omega = 5.0$

N	$e(u)$	$r(u)$	$e(\sigma)$	$r(\sigma)$	e	r	$e_0(u)$	r_0	e/η
36	1.281e+00	—	1.557e+00	—	2.016e+00	—	2.695e-01	—	0.3241
144	1.243e+00	0.0432	7.348e-01	1.0837	1.444e+00	0.4818	1.152e-01	1.2261	0.3241
576	5.392e-01	1.2048	3.438e-01	1.0958	6.395e-01	1.1749	3.902e-02	1.5618	0.1962
2304	2.519e-01	1.0980	1.690e-01	1.0248	3.033e-01	1.0761	1.116e-02	1.8054	0.1992
9216	1.232e-01	1.0314	8.463e-02	0.9975	1.495e-01	1.0207	2.937e-03	1.9266	0.1989
36864	6.131e-02	1.0073	4.255e-02	0.9919	7.463e-02	1.0024	7.496e-04	1.9702	0.1989
147456	3.063e-02	1.0012	2.137e-02	0.9939	3.735e-02	0.9988	1.891e-04	1.9869	0.1992

Table 5.7. Example 1: uniform refinement with $\omega = 10.0$

N	$e(u)$	$r(u)$	$e(\sigma)$	$r(\sigma)$	e	r	$e_0(u)$	r_0	e/η
36	1.271e+00	—	1.723e+00	—	2.142e+00	—	1.658e-01	—	0.1011
144	2.157e+00	—	1.060e+00	0.7011	2.403e+00	—	1.316e-01	0.3341	0.1011
576	1.087e+00	0.9887	9.812e-01	0.1115	1.464e+00	0.7148	9.640e-02	0.4486	0.2300
2304	1.635e+00	—	1.624e+00	—	2.305e+00	—	1.623e-01	—	0.3659
9216	3.455e-01	2.2430	3.343e-01	2.2804	4.808e-01	2.2613	3.227e-02	2.3304	0.8365
36864	8.072e-02	2.0977	6.767e-02	2.3047	1.053e-01	2.1904	5.248e-03	2.6206	0.5980
147456	3.289e-02	1.2952	2.451e-02	1.4649	4.102e-02	1.3605	1.198e-03	2.1305	0.2800

Table 5.8. Example 1: uniform refinement with $\omega = 15.0$

N	$e(u)$	$r(u)$	$e(\sigma)$	$r(\sigma)$	e	r	$e_0(u)$	r_0	e/η
36	1.088e+00	—	1.348e+00	—	1.733e+00	—	8.429e-02	—	0.0802
144	1.297e+00	—	1.393e+00	—	1.903e+00	—	1.032e-01	—	0.0802
576	5.437e-01	1.2539	3.563e-01	1.9672	6.500e-01	1.5497	1.906e-02	2.4368	0.1388
2304	2.469e-01	1.1390	1.644e-01	1.1153	2.967e-01	1.1318	3.875e-03	2.2987	0.2014
9216	1.227e-01	1.0093	8.409e-02	0.9677	1.487e-01	0.9963	1.036e-03	1.9036	0.1980
36864	6.124e-02	1.0021	4.249e-02	0.9846	7.454e-02	0.9965	2.711e-04	1.9338	0.1990
147456	3.062e-02	1.0000	2.136e-02	0.9923	3.733e-02	0.9975	6.901e-05	1.9739	0.1993

Table 5.9. Example 2: uniform refinement with $\omega = 1$

N	$e(u)$	$r(u)$	$e(\sigma)$	$r(\sigma)$	e	r	$e_0(u)$	r_0	e/η
54	3.295e+01	—	2.298e+01	—	4.017e+01	—	5.900e+00	—	0.1517
216	2.394e+01	0.4607	1.498e+01	0.6174	2.824e+01	0.5084	2.044e+00	1.5296	0.1517
864	1.514e+01	0.6607	7.545e+00	0.9893	1.692e+01	0.7391	5.490e-01	1.8961	0.1508
3456	8.927e+00	0.7624	2.996e+00	1.3324	9.417e+00	0.8453	1.417e-01	1.9540	0.1536
13824	4.908e+00	0.8631	9.685e-01	1.6294	5.003e+00	0.9125	3.821e-02	1.8908	0.1622
55296	2.555e+00	0.9421	3.991e-01	1.2791	2.586e+00	0.9522	1.025e-02	1.8980	0.1692
221184	1.295e+00	0.9800	2.632e-01	0.6005	1.322e+00	0.9682	2.706e-03	1.9219	0.1724

Table 5.10. Example 2: uniform refinement with $\omega = 10$

N	$e(u)$	$r(u)$	$e(\sigma)$	$r(\sigma)$	e	r	$e_0(u)$	r_0	e/η
54	1.823e+02	—	2.847e+02	—	3.381e+02	—	3.045e+01	—	0.0750
216	2.731e+01	2.7389	3.183e+01	3.1611	4.194e+01	3.0110	4.045e+00	2.9122	0.0750
864	2.440e+01	0.1625	1.787e+01	0.8325	3.025e+01	0.4715	1.627e+00	1.3140	0.1806
3456	2.426e+01	0.0084	2.212e+01	—	3.283e+01	—	2.200e+00	—	0.1961
13824	4.926e+00	2.3001	1.027e+00	4.4286	5.032e+00	2.7058	4.858e-02	5.5011	0.4282
55296	2.559e+00	0.9448	4.165e-01	1.3019	2.593e+00	0.9566	1.548e-02	1.6499	0.1701
221184	1.296e+00	0.9814	2.664e-01	0.6447	1.323e+00	0.9704	4.894e-03	1.6611	0.1730

Table 5.11. Example 2: uniform refinement with $\omega = 15.0$

N	$e(u)$	$r(u)$	$e(\sigma)$	$r(\sigma)$	e	r	$e_0(u)$	r_0	e/η
54	1.384e+01	—	2.487e+01	—	2.847e+01	—	1.864e+00	—	0.0429
216	1.190e+02	—	1.661e+02	—	2.043e+02	—	1.168e+01	—	0.0429
864	3.577e+01	1.7334	3.391e+01	2.2927	4.929e+01	2.0515	2.264e+00	2.3669	0.0989
3456	1.055e+01	1.7613	6.061e+00	2.4840	1.217e+01	2.0181	3.680e-01	2.6212	0.1595
13824	4.966e+00	1.0873	1.174e+00	2.3679	5.103e+00	1.2537	5.623e-02	2.7103	0.1881
55296	2.564e+00	0.9536	4.419e-01	1.4098	2.602e+00	0.9718	1.604e-02	1.8092	0.1720
221184	1.296e+00	0.9841	2.679e-01	0.7220	1.324e+00	0.9750	4.245e-03	1.9181	0.1737

Table 5.12. Example 3: uniform refinement with $\omega = 1$

N	$e(u)$	$r(u)$	$e(\sigma)$	$r(\sigma)$	e	r	$e_0(u)$	r_0	e/η
54	2.918e-01	—	2.214e-01	—	3.662e-01	—	3.455e-02	—	0.1911
216	2.159e-01	0.4346	1.337e-01	0.7274	2.539e-01	0.5284	1.442e-02	1.2603	0.1911
864	1.467e-01	0.5574	8.440e-02	0.6637	1.692e-01	0.5853	5.906e-03	1.2881	0.1874
3456	9.596e-02	0.6123	5.398e-02	0.6450	1.101e-01	0.6203	2.111e-03	1.4841	0.1859
13824	6.180e-02	0.6347	3.441e-02	0.6497	7.073e-02	0.6383	7.442e-04	1.5042	0.1794
55296	3.946e-02	0.6473	2.185e-02	0.6551	4.510e-02	0.6491	2.657e-04	1.4860	0.1702
221184	2.506e-02	0.6548	1.384e-02	0.6591	2.863e-02	0.6558	9.689e-05	1.4554	0.1595

Table 5.13. Example 3: uniform refinement with $\omega = 10.0$

N	$e(u)$	$r(u)$	$e(\sigma)$	$r(\sigma)$	e	r	$e_0(u)$	r_0	e/η
54	5.118e-01	—	6.493e-01	—	8.268e-01	—	7.391e-02	—	0.0747
216	3.680e-01	0.4760	3.521e-01	0.8830	5.093e-01	0.6990	3.794e-02	0.9621	0.0747
864	1.614e-01	1.1891	1.042e-01	1.7561	1.921e-01	1.4065	7.287e-03	2.3803	0.1592
3456	9.701e-02	0.7342	5.493e-02	0.9243	1.115e-01	0.7851	1.728e-03	2.0761	0.1997
13824	6.192e-02	0.6477	3.446e-02	0.6725	7.087e-02	0.6536	4.796e-04	1.8494	0.1818
55296	3.948e-02	0.6494	2.186e-02	0.6568	4.512e-02	0.6512	1.547e-04	1.6318	0.1705
221184	2.507e-02	0.6553	1.384e-02	0.6594	2.863e-02	0.6562	5.335e-05	1.5362	0.1596

Table 5.14. Example 3: uniform refinement with $\omega = 15$

N	$e(u)$	$r(u)$	$e(\sigma)$	$r(\sigma)$	e	r	$e_0(u)$	r_0	e/η
54	3.665e-01	—	7.394e-01	—	8.252e-01	—	5.125e-02	—	0.0479
216	5.089e+00	—	7.604e+00	—	9.150e+00	—	5.319e-01	—	0.0479
864	2.585e-01	4.2995	1.793e-01	5.4060	3.146e-01	4.8623	1.364e-02	5.2850	0.0992
3456	1.564e-01	0.7244	1.270e-01	0.4985	2.015e-01	0.6429	7.878e-03	0.7923	0.2020
13824	6.458e-02	1.2765	3.874e-02	1.7122	7.531e-02	1.4197	1.281e-03	2.6203	0.2791
55296	3.956e-02	0.7070	2.200e-02	0.8166	4.526e-02	0.7344	2.157e-04	2.5704	0.1810
221184	2.507e-02	0.6578	1.385e-02	0.6679	2.864e-02	0.6602	5.689e-05	1.9229	0.1600

Table 5.15. Example 2: hybrid adaptive refinement with $\omega = 1.0$

N	$e(u)$	$r(u)$	$e(\sigma)$	$r(\sigma)$	e	r	e/η
54	3.295e+01	—	2.298e+01	—	4.017e+01	—	0.1517
216	2.394e+01	0.4607	1.498e+01	0.6174	2.824e+01	0.5084	0.1517
252	2.148e+01	1.4097	9.065e+00	6.5157	2.331e+01	2.4891	0.1508
270	1.812e+01	4.9215	7.802e+00	4.3518	1.973e+01	4.8339	0.1495
378	1.233e+01	2.2903	4.207e+00	3.6715	1.303e+01	2.4682	0.1719
414	1.119e+01	2.1266	4.183e+00	0.1236	1.195e+01	1.8998	0.1566
630	6.986e+00	2.2446	2.113e+00	3.2540	7.298e+00	2.3476	0.1859
828	5.371e+00	1.9239	1.394e+00	3.0423	5.549e+00	2.0055	0.1679
1134	4.041e+00	1.8098	1.248e+00	0.7059	4.229e+00	1.7275	0.1735
2070	2.901e+00	1.1010	8.147e-01	1.4161	3.013e+00	1.1262	0.1709
3222	2.429e+00	0.8037	9.596e-01	—	2.611e+00	0.6474	0.1723
6732	1.611e+00	1.1141	5.239e-01	1.6426	1.694e+00	1.1746	0.1919
12456	1.197e+00	0.9653	4.504e-01	0.4914	1.279e+00	0.9135	0.1839
23364	8.526e-01	1.0789	3.089e-01	1.1988	9.069e-01	1.0933	0.1873
46521	6.143e-01	0.9518	2.382e-01	0.7550	6.589e-01	0.9275	0.1855
89235	4.229e-01	1.1467	1.447e-01	1.5297	4.470e-01	1.1917	0.1876
173520	3.117e-01	0.9170	1.201e-01	0.5622	3.341e-01	0.8756	0.1799
328185	2.212e-01	1.0765	7.958e-02	1.2905	2.351e-01	1.1026	0.1847

Table 5.16. Example 2: hybrid adaptive refinement with $\omega = 10.0$

N	$e(u)$	$r(u)$	$e(\sigma)$	$r(\sigma)$	e	r	e/η
54	1.823e+02	—	2.847e+02	—	3.381e+02	—	0.0750
216	2.731e+01	2.7389	3.183e+01	3.1611	4.194e+01	3.0110	0.0750
864	2.440e+01	0.1625	1.787e+01	0.8325	3.025e+01	0.4715	0.1806
3456	2.426e+01	0.0084	2.212e+01	—	3.283e+01	—	0.1961
13824	4.926e+00	2.3001	1.027e+00	4.4286	5.032e+00	2.7058	0.4282
14112	3.962e+00	21.1095	1.432e+00	—	4.213e+00	17.2184	0.1701
14544	2.880e+00	21.1550	9.110e-01	30.0031	3.021e+00	22.0647	0.1873
15696	2.321e+00	5.6609	9.138e-01	—	2.495e+00	5.0216	0.1765
18558	1.594e+00	4.4874	5.338e-01	6.4195	1.681e+00	4.7131	0.1935
23922	1.185e+00	2.3332	4.509e-01	1.3300	1.268e+00	2.2196	0.1856
34290	8.409e-01	1.9078	3.043e-01	2.1842	8.942e-01	1.9412	0.1891
56304	6.103e-01	1.2927	2.361e-01	1.0224	6.544e-01	1.2595	0.1858
97893	4.209e-01	1.3435	1.439e-01	1.7920	4.448e-01	1.3960	0.1878
171693	3.176e-01	1.0021	1.217e-01	0.5945	3.401e-01	0.9548	0.1800
324936	2.243e-01	1.0903	8.097e-02	1.2783	2.385e-01	1.1132	0.1844

Table 5.17. Example 2: hybrid adaptive refinement with $\omega = 15.0$

N	$e(u)$	$r(u)$	$e(\sigma)$	$r(\sigma)$	e	r	e/η
54	1.384e+01	—	2.487e+01	—	2.847e+01	—	0.0429
216	1.190e+02	—	1.661e+02	—	2.043e+02	—	0.0429
864	3.577e+01	1.7334	3.391e+01	2.2927	4.929e+01	2.0515	0.0989
3456	1.055e+01	1.7613	6.061e+00	2.4840	1.217e+01	2.0181	0.1595
13824	4.966e+00	1.0873	1.174e+00	2.3679	5.103e+00	1.2537	0.1881
55296	2.564e+00	0.9536	4.419e-01	1.4098	2.602e+00	0.9718	0.1720
55872	2.157e+00	33.3993	7.913e-01	—	2.297e+00	24.0356	0.1737
57888	1.553e+00	18.5436	5.102e-01	24.7643	1.634e+00	19.2139	0.1891
62514	1.162e+00	7.5468	4.379e-01	3.9739	1.241e+00	7.1521	0.1857
72018	8.300e-01	4.7507	3.008e-01	5.3071	8.828e-01	4.8176	0.1895
93294	6.016e-01	2.4863	2.337e-01	1.9524	6.454e-01	2.4204	0.1865
133092	4.181e-01	2.0485	1.441e-01	2.7202	4.423e-01	2.1279	0.1880
214128	3.087e-01	1.2754	1.188e-01	0.8123	3.308e-01	1.2211	0.1806
364752	2.196e-01	1.2801	7.895e-02	1.5345	2.333e-01	1.3110	0.1848

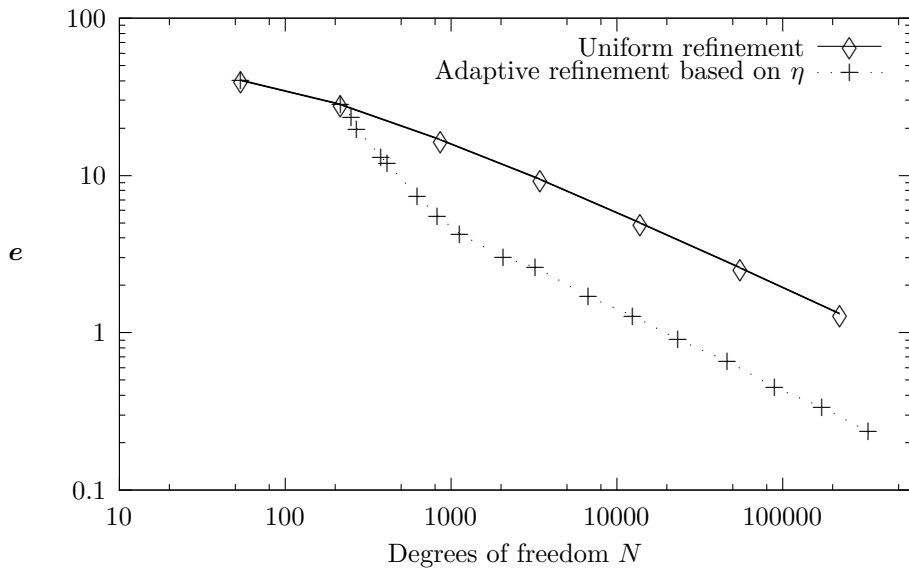


Figure 5.1. Example 2: Global error for the uniform and adaptive refinements, with $\omega = 1.0$

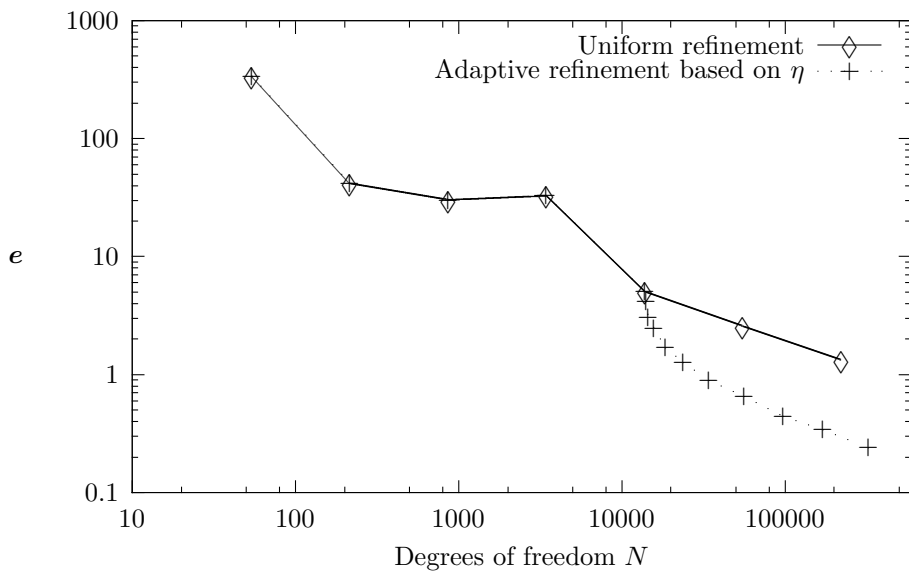


Figure 5.2. Example 2: Global error for the uniform and adaptive refinements, with $\omega = 10.0$

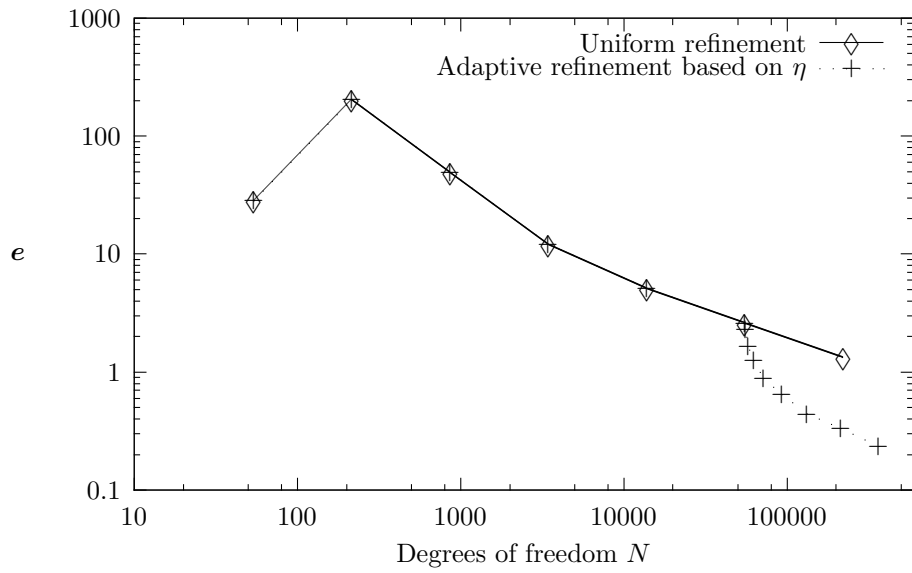


Figure 5.3. Example 2: Global error for the uniform and adaptive refinements, with $\omega = 15.0$

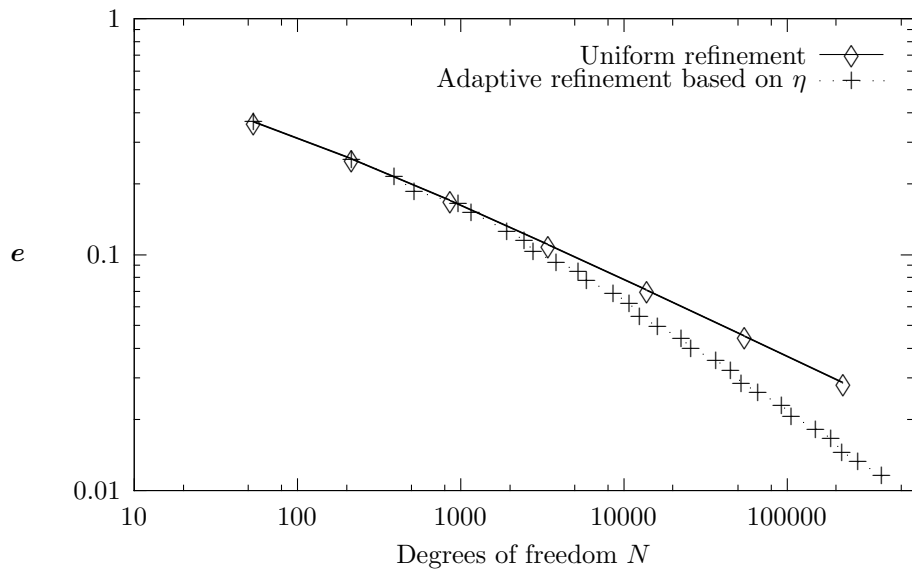


Figure 5.4. Example 3: Global error for the uniform and adaptive refinements, with $\omega = 1.0$

Table 5.18. Example 3: hybrid adaptive refinement with $\omega = 1.0$

N	$e(u)$	$r(u)$	$e(\sigma)$	$r(\sigma)$	e	r	e/η
54	2.918e-01	—	2.214e-01	—	3.662e-01	—	0.1911
216	2.159e-01	0.4346	1.337e-01	0.7274	2.539e-01	0.5284	0.1911
396	1.852e-01	0.5055	1.053e-01	0.7868	2.131e-01	0.5788	0.1874
522	1.616e-01	0.9852	9.330e-02	0.8786	1.866e-01	0.9588	0.1961
972	1.455e-01	0.3389	7.630e-02	0.6472	1.643e-01	0.4106	0.2035
1170	1.346e-01	0.8402	6.947e-02	1.0118	1.514e-01	0.8768	0.2102
1944	1.119e-01	0.7271	5.717e-02	0.7677	1.257e-01	0.7355	0.2206
2466	1.014e-01	0.8291	5.385e-02	0.5030	1.148e-01	0.7595	0.2147
2808	9.128e-02	1.6173	4.757e-02	1.9085	1.029e-01	1.6804	0.2214
3879	8.223e-02	0.6467	4.229e-02	0.7288	9.246e-02	0.6641	0.2175
5274	7.613e-02	0.5016	3.860e-02	0.5933	8.536e-02	0.5206	0.2166
5958	6.952e-02	1.4879	3.478e-02	1.7080	7.774e-02	1.5324	0.2276
8676	6.167e-02	0.6376	3.015e-02	0.7605	6.865e-02	0.6617	0.2288
10854	5.568e-02	0.9127	2.698e-02	0.9938	6.187e-02	0.9282	0.2266
12564	4.928e-02	1.6706	2.348e-02	1.8985	5.458e-02	1.7133	0.2317
16227	4.478e-02	0.7481	2.147e-02	0.6976	4.966e-02	0.7387	0.2248
22662	3.965e-02	0.7290	1.962e-02	0.5405	4.424e-02	0.6928	0.2248
25794	3.602e-02	1.4803	1.761e-02	1.6728	4.010e-02	1.5178	0.2300
36684	3.199e-02	0.6750	1.556e-02	0.7024	3.557e-02	0.6802	0.2313
45513	2.922e-02	0.8390	1.408e-02	0.9262	3.244e-02	0.8556	0.2313
52974	2.565e-02	1.7156	1.266e-02	1.4056	2.860e-02	1.6561	0.2385
67023	2.330e-02	0.8173	1.140e-02	0.8861	2.594e-02	0.8307	0.2320
93411	2.049e-02	0.7751	1.021e-02	0.6641	2.289e-02	0.7534	0.2306
107127	1.853e-02	1.4647	9.185e-03	1.5486	2.068e-02	1.4813	0.2343
151002	1.632e-02	0.7391	8.116e-03	0.7209	1.823e-02	0.7355	0.2359
186462	1.494e-02	0.8394	7.313e-03	0.9875	1.664e-02	0.8684	0.2349
217863	1.301e-02	1.7801	6.421e-03	1.6707	1.451e-02	1.7588	0.2417
272781	1.190e-02	0.7941	5.880e-03	0.7830	1.327e-02	0.7919	0.2342
381510	1.032e-02	0.8472	5.207e-03	0.7253	1.156e-02	0.8229	0.2338

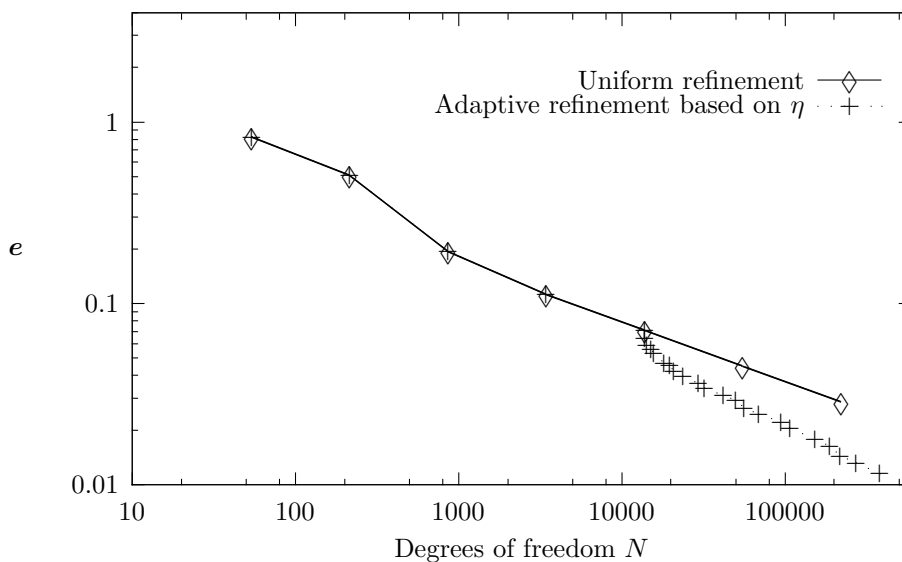


Figure 5.5. Example 3: Global error for the uniform and adaptive refinements, with $\omega = 10.0$

Table 5.19. Example 3: hybrid adaptive refinement with $\omega = 10.0$

N	$e(u)$	$r(u)$	$e(\sigma)$	$r(\sigma)$	e	r	e/η
54	5.118e-01	—	6.493e-01	—	8.268e-01	—	0.0747
216	3.680e-01	0.4760	3.521e-01	0.8830	5.093e-01	0.6990	0.0747
864	1.614e-01	1.1891	1.042e-01	1.7561	1.921e-01	1.4065	0.1592
3456	9.701e-02	0.7342	5.493e-02	0.9243	1.115e-01	0.7851	0.1997
13824	6.192e-02	0.6477	3.446e-02	0.6725	7.087e-02	0.6536	0.1818
13878	5.678e-02	44.5216	2.910e-02	86.7418	6.380e-02	53.8964	0.1705
14238	5.240e-02	6.2688	2.698e-02	5.9135	5.893e-02	6.1946	0.1616
15219	5.031e-02	1.2211	2.402e-02	3.4895	5.575e-02	1.6689	0.1585
15732	4.789e-02	2.9773	2.288e-02	2.9285	5.307e-02	2.9682	0.1714
18162	4.209e-02	1.7974	2.068e-02	1.4101	4.689e-02	1.7238	0.1802
19800	4.077e-02	0.7344	2.023e-02	0.5030	4.552e-02	0.6890	0.1806
20898	3.808e-02	2.5292	1.843e-02	3.4467	4.231e-02	2.7069	0.1943
23814	3.576e-02	0.9616	1.684e-02	1.3861	3.953e-02	1.0404	0.1935
29538	3.258e-02	0.8666	1.539e-02	0.8359	3.603e-02	0.8610	0.1944
32004	3.099e-02	1.2446	1.433e-02	1.7798	3.414e-02	1.3405	0.2024
42012	2.805e-02	0.7329	1.286e-02	0.7975	3.086e-02	0.7442	0.2085
49941	2.649e-02	0.6629	1.223e-02	0.5777	2.918e-02	0.6480	0.2102
56385	2.396e-02	1.6524	1.118e-02	1.4819	2.644e-02	1.6222	0.2209
69525	2.225e-02	0.7070	1.033e-02	0.7525	2.453e-02	0.7151	0.2186
95067	2.002e-02	0.6762	9.381e-03	0.6163	2.211e-02	0.6655	0.2198
107829	1.850e-02	1.2523	8.711e-03	1.1776	2.045e-02	1.2388	0.2268
152721	1.605e-02	0.8146	7.615e-03	0.7725	1.777e-02	0.8069	0.2315
188208	1.471e-02	0.8365	7.045e-03	0.7451	1.631e-02	0.8196	0.2294
218754	1.293e-02	1.7198	6.331e-03	1.4208	1.439e-02	1.6630	0.2369
273780	1.184e-02	0.7842	5.865e-03	0.6810	1.321e-02	0.7641	0.2318
382905	1.026e-02	0.8524	5.190e-03	0.7291	1.150e-02	0.8277	0.2323

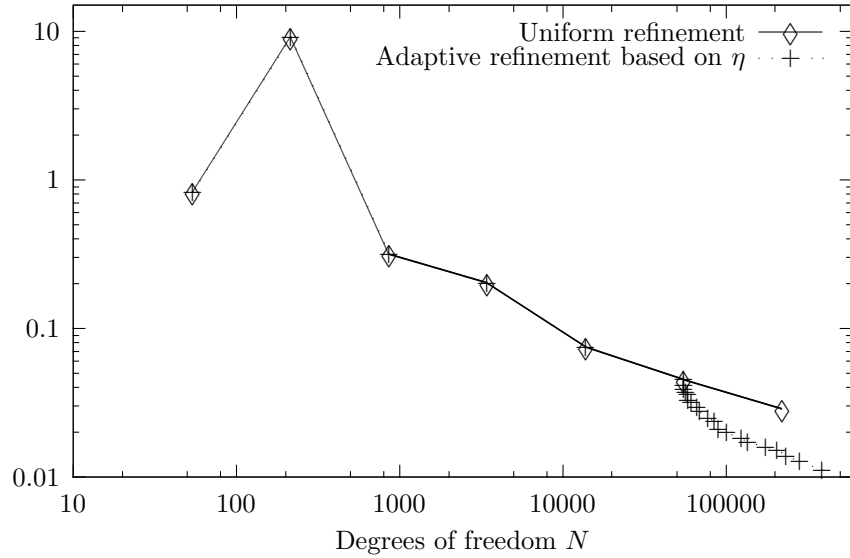


Figure 5.6. Example 3: Global error for the uniform and adaptive refinements, with $\omega = 15.0$

Table 5.20. Example 3: hybrid adaptive refinement with $\omega = 15.0$

N	$e(u)$	$r(u)$	$e(\sigma)$	$r(\sigma)$	e	r	e/η
54	3.665e-01	—	7.394e-01	—	8.252e-01	—	0.0479
216	5.089e+00	—	7.604e+00	—	9.150e+00	—	0.0479
864	2.585e-01	4.2995	1.793e-01	5.4060	3.146e-01	4.8623	0.0992
3456	1.564e-01	0.7244	1.270e-01	0.4985	2.015e-01	0.6429	0.2020
13824	6.458e-02	1.2765	3.874e-02	1.7122	7.531e-02	1.4197	0.2791
55296	3.956e-02	0.7070	2.200e-02	0.8166	4.526e-02	0.7344	0.1810
55350	3.667e-02	155.5654	1.924e-02	274.7426	4.141e-02	182.4908	0.1600
55404	3.437e-02	132.4926	1.866e-02	62.6713	3.911e-02	117.0130	0.1529
56808	3.331e-02	2.5103	1.731e-02	6.0037	3.754e-02	3.2790	0.1474
58185	3.162e-02	4.3581	1.679e-02	2.5333	3.580e-02	3.9634	0.1558
59085	2.885e-02	11.9475	1.567e-02	8.9721	3.283e-02	11.2811	0.1683
61578	2.787e-02	1.6716	1.561e-02	0.2008	3.194e-02	1.3284	0.1670
66816	2.600e-02	1.6995	1.415e-02	2.4048	2.960e-02	1.8643	0.1736
68994	2.442e-02	3.9088	1.289e-02	5.8062	2.761e-02	4.3324	0.1837
77976	2.224e-02	1.5276	1.144e-02	1.9558	2.501e-02	1.6190	0.1882
85212	2.110e-02	1.1850	1.058e-02	1.7558	2.360e-02	1.3021	0.1892
90324	1.899e-02	3.6171	8.936e-03	5.7985	2.099e-02	4.0337	0.1986
101547	1.802e-02	0.8974	8.402e-03	1.0516	1.988e-02	0.9251	0.1915
125163	1.649e-02	0.8449	7.658e-03	0.8872	1.819e-02	0.8525	0.1943
135999	1.553e-02	1.4469	7.239e-03	1.3554	1.714e-02	1.4307	0.2025
175401	1.435e-02	0.6235	6.893e-03	0.3850	1.592e-02	0.5798	0.2095
207495	1.364e-02	0.5987	6.761e-03	0.2306	1.523e-02	0.5279	0.2157
233838	1.237e-02	1.6463	6.280e-03	1.2333	1.387e-02	1.5633	0.2292
284310	1.139e-02	0.8454	5.567e-03	1.2338	1.267e-02	0.9227	0.2284
388269	1.008e-02	0.7805	4.770e-03	0.9917	1.115e-02	0.8202	0.2255

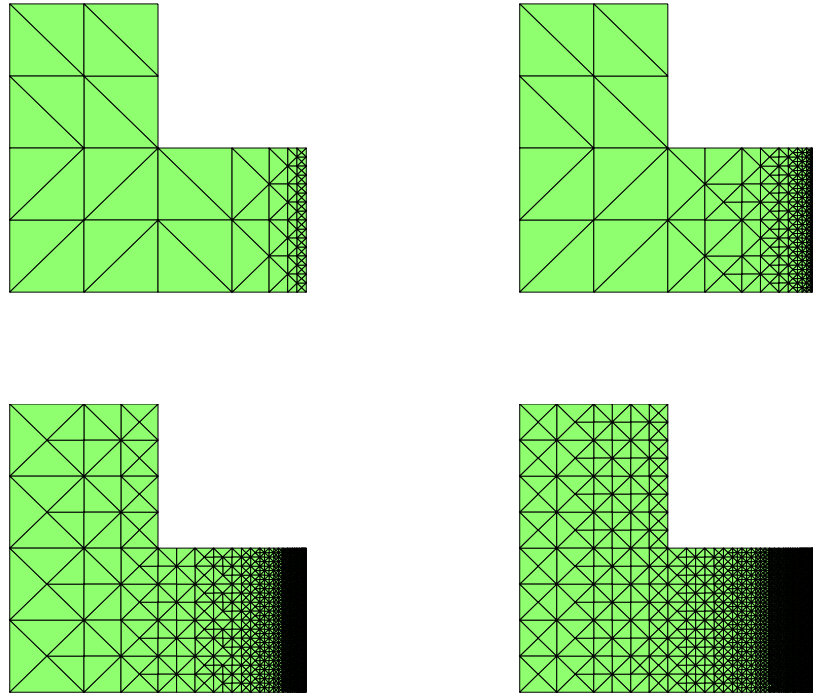


Figure 5.7: Adapted intermediate meshes with 1134, 6732, 46521 and 173520 dof (Example 2, using $\omega = 1.0$).

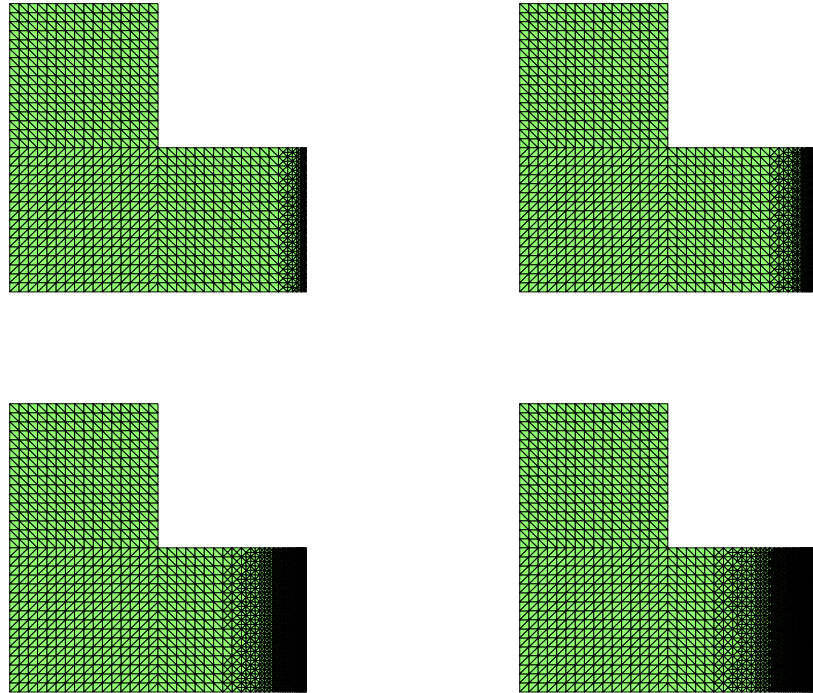


Figure 5.8: Adapted intermediate meshes with 18558, 34290, 97893 and 171693 dof (Example 2, using $\omega = 10.0$).

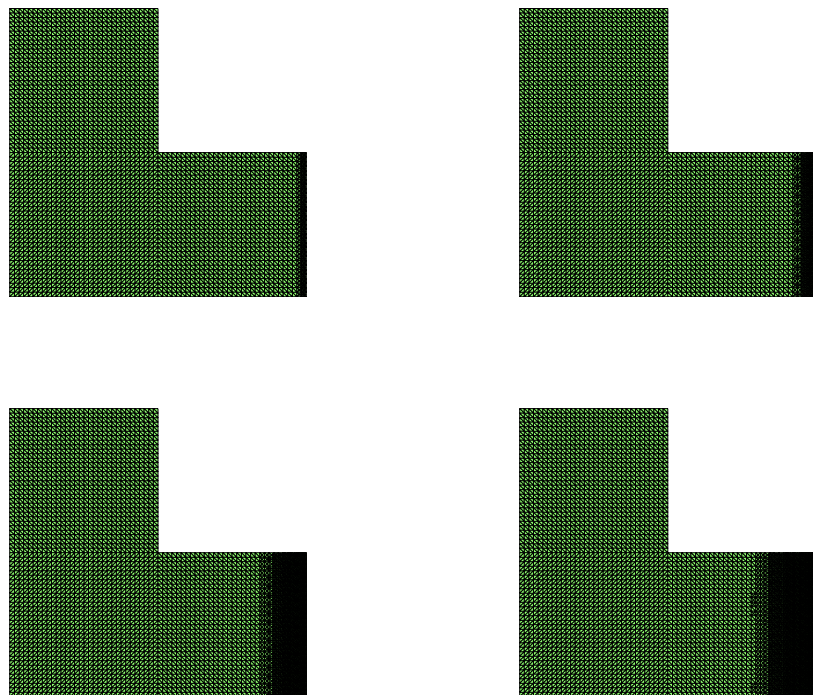


Figure 5.9: Adapted intermediate meshes with 57888, 72018, 133092 and 214128 dof (Example 2, using $\omega = 15.0$).

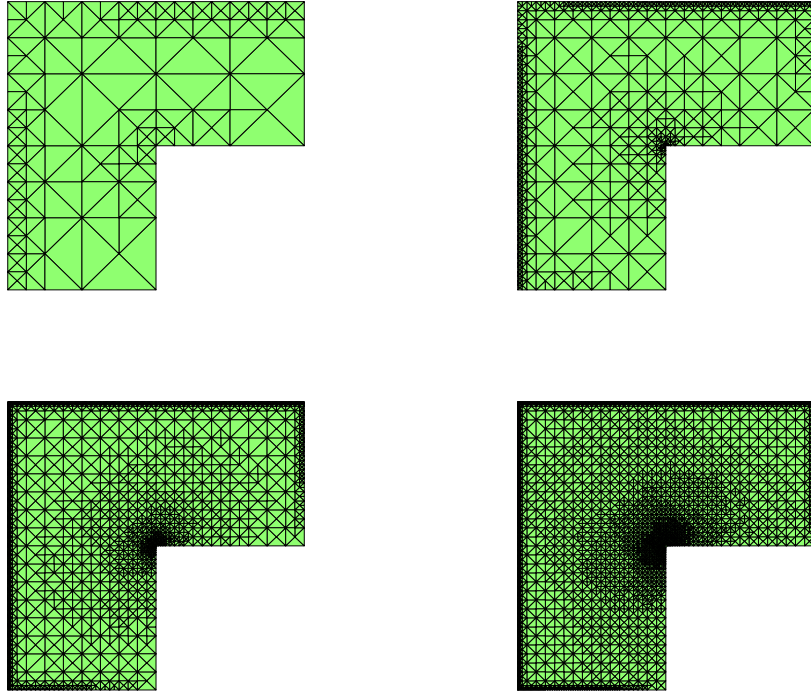


Figure 5.10: Adapted intermediate meshes with 1944, 10854, 52974 and 151002 dof (Example 3, using $\omega = 1.0$).

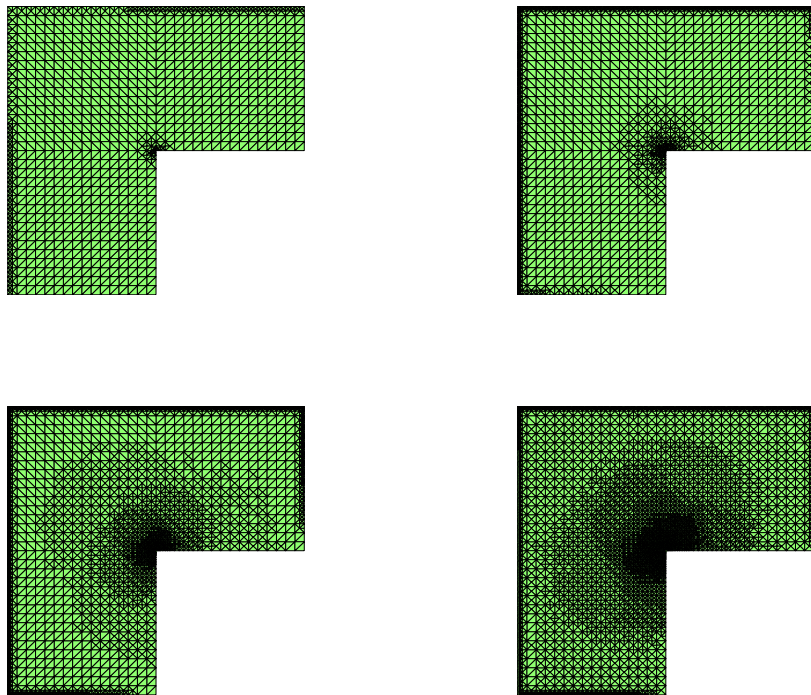


Figure 5.11: Adapted intermediate meshes with 18162, 42012, 107829 and 218754 dof (Example 3, using $\omega = 10.0$).

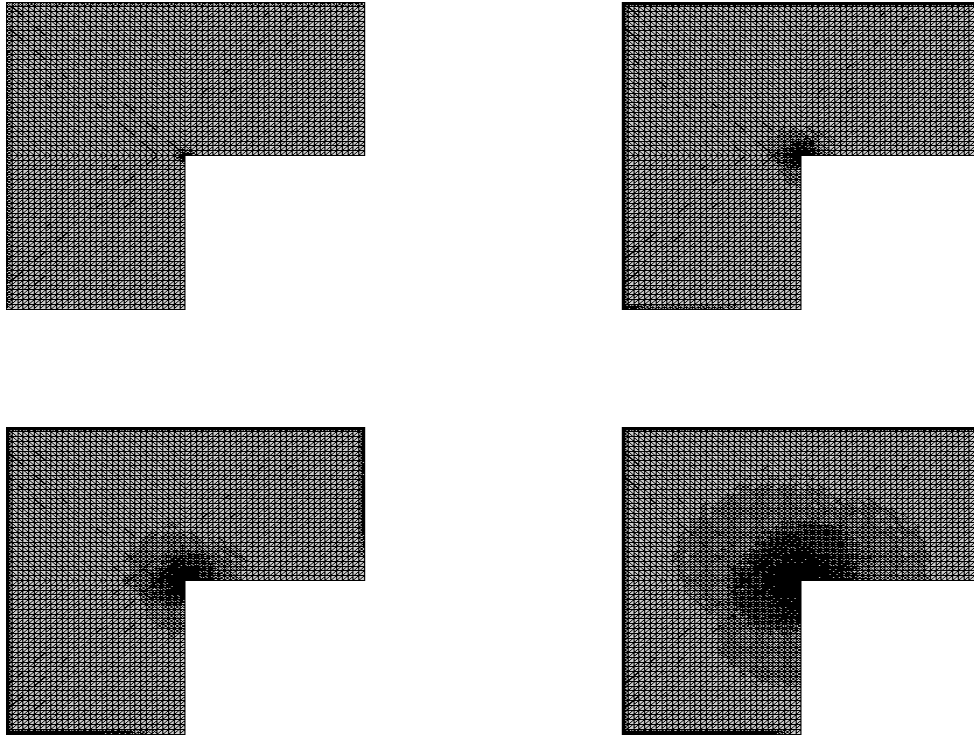


Figure 5.12: Adapted intermediate meshes with 59085, 101547, 175401 and 388269 dof (Example 3, using $\omega = 15.0$).

Acknowledgements

This work was done during short visits of R. Bustinza and T.P. Barrios to the Departamento de Ingeniería Matemática e Informática, Universidad Pública de Navarra, Campus Tudela, Spain. They wish to thank professors V. Domínguez and R. Ortega, both from this University, for the kind hospitality.

References

- [1] D.N. ARNOLD, F. BREZZI, B. COCKBURN AND L.D. MARINI: *Unified analysis of discontinuous Galerkin methods for elliptic problems*. SIAM Journal on Numerical Analysis, vol. 39, 5, pp. 1749-1779, (2001).
- [2] M. AINSWORTH: *A posteriori error estimation for discontinuous Galerkin finite element approximation*. SIAM Journal on Numerical Analysis, vol. 45, pp. 1777-1798, (2007).
- [3] T.P. BARRIOS AND R. BUSTINZA: *An augmented discontinuous Galerkin method for elliptic problems*. Comptes Rendus de l'Academie des Sciences, Series I, vol. 344, pp. 53-58, (2007).
- [4] T.P. BARRIOS AND R. BUSTINZA: *A priori and a posteriori error analyses of an augmented discontinuous Galerkin formulation*. IMA Journal of Numerical Analysis, vol 30, 4, pp. 987-1008, (2010).
- [5] T.P. BARRIOS AND R. BUSTINZA: *An a posteriori error analysis of an augmented discontinuous Galerkin formulation for Darcy flow*. Numerische Mathematik, vol 120, pp. 231-269, (2012).
- [6] R. BECKER, P. HANSBO AND M.G. LARSON: *Energy norm a posteriori error estimation for discontinuous Galerkin methods*. Computer Methods in Applied Mechanics and Engineering, vol. 192, pp. 723-733 (2003).

- [7] G. BENITEZ ALVAREZ, A.F. DOURADO LOULA, E. GOMES DUTRA DO CARMO, AND F. ALVES ROCHINHA: *A discontinuous finite element formulation for Helmholtz equation*. Computer Methods in Applied Mechanics and Engineering, vol. 195, pp. 4018-4035, (2006).
- [8] S. BRENNER: *Poincaré-Friedrichs inequalities for piecewise H^1 functions*. SIAM Journal on Numerical Analysis, vol. 41, 1, pp. 306-324, (2003).
- [9] R. BUSTINZA AND G.N. GATICA: *A local discontinuous Galerkin method for nonlinear diffusion problems with mixed boundary conditions*. SIAM Journal on Scientific Computing, vol. 26, 1, pp. 152-177, (2004).
- [10] R. BUSTINZA, G.N. GATICA AND B. COCKBURN: *An a-posteriori error estimate for the local discontinuous Galerkin method applied to linear and nonlinear diffusion problems*. Journal of Scientific Computing, vol. 22, 1, pp. 147-185, (2005).
- [11] P. CASTILLO, B. COCKBURN, I. PERUGIA, AND D. SCHÖTZAU: *An a priori error analysis of the local discontinuous Galerkin method for elliptic problems*. SIAM Journal on Numerical Analysis, vol. 38, 5, pp. 1676-1706, (2000).
- [12] O. CESSENAT, AND B. DEPRES: *Application of an ultra weak variational formulation of elliptic PDEs to the two-dimensional Helmholtz problem*. SIAM Journal on Numerical Analysis, vol. 35, pp. 255-299, (1998).
- [13] P. CIARLET: *The Finite Element Method for Elliptic Problems*. North-Holland, Amsterdam, (1978).
- [14] M. DAUGE: *Elliptic boundary value problems on corner domains*. Lecture Notes in Mathematics, vol. 1341. Springer-Verlag, Berlin, (1988).
- [15] B. ENGQUIST AND A. MAJDA: *Radiation boundary conditions for acoustic and elastic wave calculations*. Communications on Pure and Applied Mathematics, vol. 32, 3, pp. 314-358, (1979).
- [16] C. FARHAT, I. HARARI AND L. FRANCA: *The discontinuous enrichment method*. Computer Methods in Applied Mechanics and Engineering, vol. 190, pp. 6455-6479, (2001).
- [17] C. FARHAT, I. HARARI AND U. HETMANIUK: *A discontinuous Galerkin method with Lagrange multipliers for the solution of Helmholtz problem in the mid-frequency regime*. Computer Methods in Applied Mechanics and Engineering, vol. 192, pp. 1389-1419, (2003).
- [18] X. FENG AND H. WU: *Discontinuous Galerkin methods for the Helmholtz equation with large wave number*. SIAM Journal on Numerical Analysis, col. 47, 4, pp. 2872-2896, (2009).
- [19] X. FENG AND H. WU: *hp-discontinuous Galerkin methods for the Helmholtz equation with large wave number*. Mathematics of Computation, vol. 80, 276, pp.1997-2024, (2011)
- [20] X. FENG AND Y. XING: *Absolutely stable local discontinuous Galerkin methods for the Helmholtz equation with large wave number*. Mathematics of Computation, vol. 82, 283, pp. 1269-1296, (2013).
- [21] G.N. GATICA AND F.J. SAYAS: *A note on the local approximation properties of piecewise polynomials with applications to LDG methods*. Complex Variables and Elliptic Equations, vol. 51, 2, pp. 109-117, (2006).
- [22] V. GIRAULT AND P.A. RAVIART: *Finite Element Methods for Navier-Stokes Equations: Theory and Algorithms*. Springer Series in Computational Mathematics, 1986.
- [23] C.J. GITTELSON, R. HITMAIR AND I. PERUGIA: *Plane wave discontinuous Galerkin methods: Analysis of the h-version*. M2AN, Mathematical Modelling and Numerical Analysis, vol. 43, pp. 297-331, (2009).
- [24] C.I. GOLSTEIN: *The weak element method applied to Helmholtz type equations*. Applied Numerical Mathematics, vol. 2, pp. 409-426, (1986).

- [25] P. GRISVARD: *Elliptic Problems in Nonsmooth Domains*. Pitman, (1985).
- [26] R. HIPTMAIR AND I. PERUGIA: *Mixed plane wave discontinuous Galerkin methods*. Lecture Notes in Computational Science and Engineering, vol. 70, pp. 51-62, (2009).
- [27] R.H.W. HOPPE AND N. SHARMA: *Convergence analysis of an adaptive interior penalty discontinuous Galerkin method for the Helmholtz equation*. IMA Journal of Numerical Analysis, vol. 33, 3, pp. 898-921, (2013).
- [28] P. HOUSTON, I. PERUGIA, A. SCHNEEBELI AND D. SCHÖTZAU: *Mixed discontinuous Galerkin approximation of the Maxwell operator: the indefinite case*. M2AN, Mathematical Modelling and Numerical Analysis, vol. 39, 4, pp. 727-753, (2005).
- [29] P. HOUSTON, D. SCHÖTZAU AND T.P. WIHLE: *Energy norm a posteriori error estimation of hp-adaptive discontinuous Galerkin methods for elliptic problems*. Mathematical Models Methods in Applied Science, vol. 17, pp. 33-62, (2007).
- [30] T.J.R. HUGHES, A. MASUD AND J. WAN: *A stabilized mixed discontinuous Galerkin method for Darcy flow*. Computer Methods in Applied Mechanics and Engineering, vol. 195, 25-28, pp. 3347-3381, (2006).
- [31] F. IHLENBURG: *Finite Element Analysis of Acoustic Scattering*. Applied Mathematical Sciences, vol. 132, Springer-Verlag, New York, (1998).
- [32] O. KARAKASHIAN AND F. PASCAL: *A posteriori error estimates for a discontinuous Galerkin approximation of second order elliptic problems*. SIAM Journal on Numerical Analysis, vol. 45, pp. 641-665, (2003).
- [33] C. LOVADINA AND L.D. MARINI: *A-Posteriori Error Estimates for Discontinuous Galerkin Approximations of Second Order Elliptic Problems*. Journal of Scientific Computing, vol. 40, pp. 340-359, (2009).
- [34] A.F. DOURADO LOULA, G. BENITEZ ALVAREZ, E. GOMES DUTRA DO CARMO AND F. ALVES ROCHINHA: *A discontinuous finite element method at element level for Helmholtz equation*. Computer Methods in Applied Mechanics and Engineering, vol. 196, pp. 867-878, (2007).
- [35] P. MONK AND DA-QING WANG: *A least-squares method for Helmholtz equation*. Computer Methods in Applied Mechanics and Engineering, vol. 175, pp. 121-136, (1999).
- [36] I. PERUGIA AND D. SCHÖTZAU: *An hp-analysis of the local discontinuous Galerkin method for diffusion problems*. Journal of Scientific Computing, vol. 17, pp. 561-571, (2002).
- [37] B. RIVIERE AND M.F. WHEELER: *A posteriori error estimates for discontinuous Galerkin methods applied to elliptic problems*. Computers and Mathematics with Applications, vol. 46, pp. 141-164, (2003).
- [38] A.H. SCHATZ: *An observation concerning Ritz-Galerkin methods with indefinite bilinear forms*. Mathematics of Computation, vol. 28, 128, pp. 959-962, (1974).
- [39] R. VERFÜRTH: *A Review of A Posteriori Error Estimation and Adaptive Mesh-Refinement Techniques*. Wiley-Teubner (Chichester), 1996.

Centro de Investigación en Ingeniería Matemática (CI²MA)

PRE-PUBLICACIONES 2013

- 2013-12 SALIM MEDDAHI, DAVID MORA, RODOLFO RODRÍGUEZ: *A finite element analysis of a pseudostress formulation for the Stokes eigenvalue problem*
- 2013-13 GABRIEL CARCAMO, FABIÁN FLORES-BAZÁN: *A geometric characterization of strong duality in nonconvex quadratic programming with linear and nonconvex quadratic constraints*
- 2013-14 RAIMUND BÜRGER, CHRISTOPHE CHALONS, LUIS M. VILLADA: *Anti-diffusive and random-sampling Lagrangian-remap schemes for the multi-class Lighthill-Whitham-Richards traffic model*
- 2013-15 FERNANDO BETANCOURT, RAIMUND BÜRGER, STEFAN DIEHL, CAMILO MEJÍAS: *Advance methods of flux identification for Clarifier-Thickener simulation models*
- 2013-16 FABIÁN FLORES-BAZÁN: *A Fritz John necessary optimality condition of the alternative-type*
- 2013-17 VERONICA ANAYA, DAVID MORA, RICARDO RUIZ-BAIER: *An augmented mixed finite element method for the vorticity-velocity-pressure formulation of the Stokes equations*
- 2013-18 FERNANDO BETANCOURT, RAIMUND BÜRGER, STEFAN DIEHL, SEBASTIAN FARÅS: *A model of clarifier-thickener control with time-dependent feed properties*
- 2013-19 GABRIEL N. GATICA, ANTONIO MARQUEZ, RICARDO OYARZÚA, RAMIRO REBOLLEDO: *Analysis of an augmented fully-mixed approach for the coupling of quasi-Newtonian fluids and porous media*
- 2013-20 SERGIO CAUCAO, DAVID MORA, RICARDO OYARZÚA: *Analysis of a mixed-FEM for the pseudostress-velocity formulation of the Stokes problem with varying density*
- 2013-21 ERWAN HINGANT, MAURICIO SEPÚLVEDA: *On a sorption-coagulation equation: statement, existence and numerical approximation*
- 2013-22 VERONICA ANAYA, MOSTAFA BENDAHMANE, MICHAEL LANGLAIS, MAURICIO SEPÚLVEDA: *A convergent finite volume method for a model of indirectly transmitted diseases with nonlocal cross-diffusion*
- 2013-23 TOMÁS BARRIOS, ROMMEL BUSTINZA, VÍCTOR DOMÍNGUEZ: *On the discontinuous Galerkin method for solving boundary problems for the Helmholtz equation: A priori and a posteriori error analyses*

Para obtener copias de las Pre-Publicaciones, escribir o llamar a: DIRECTOR, CENTRO DE INVESTIGACIÓN EN INGENIERÍA MATEMÁTICA, UNIVERSIDAD DE CONCEPCIÓN, CASILLA 160-C, CONCEPCIÓN, CHILE, TEL.: 41-2661324, o bien, visitar la página web del centro: <http://www.ci2ma.udec.cl>



**CENTRO DE INVESTIGACIÓN EN
INGENIERÍA MATEMÁTICA (CI²MA)
Universidad de Concepción**



Casilla 160-C, Concepción, Chile
Tel.: 56-41-2661324/2661554/2661316
<http://www.ci2ma.udec.cl>